Journal of Environmental Management 226 (2018) 457–475

Contents lists available at ScienceDirect

Journal of Environmental Management

journal homepage: www.elsevier.com/locate/jenvman

Research article

Thermal evaluation of urbanization using a hybrid approach

Mehdi Ketabchy, David J. Sample*, Theresa Wynn-Thompson, Mohammad Nayeb Yazdi

Department of Biological System Engineering, Virginia Polytechnic Institute and State University, United States

ARTICLE INFO

Keywords:
MINUHET
SWMM
Stream temperature
Thermal impacts
Toxicity threshold
Heat load

ABSTRACT

Urban development increases runoff temperatures from buildings and pavement, which can be harmful to aquatic life. However, our ability to predict runoff temperature as a function of land use is limited. This paper explores available tools for simulating runoff temperature with respect to brook trout (*Salvelinus* sp.), a sensitive species. The Minnesota Urban Heat Export Tool (MINUHET) and the Storm Water Management Model (SWMM) were applied to a 14.1 km^2 portion of the Stroubles Creek watershed near Blacksburg, Virginia for two summers. Streamflow, water temperature, and weather data were acquired from the Virginia Tech StREAM Lab (Stream Research, Education, and Management) monitoring stations. SWMM and MINUHET were calibrated and validated for streamflow, and stream temperature, respectively. The models were sensitive to imperviousness (SWMM-predicted streamflow) and dew point temperature (MINUHET-predicted water temperature). While the models output time-step was 15 min, the model performance in simulating streamflow was evaluated using Nash-Sutcliffe Efficiency (NSE) on hourly time-steps. NSE values were 0.67 and 0.65 for SWMM and 0.62 and 0.57 for MINUHET during the calibration and validation periods, respectively, indicating that SWMM performed better than MINUHET in streamflow simulation. Stream temperatures were simulated using MINUHET with NSE value of 0.58 for the validation period, demonstrating a satisfactory simulation of water temperature. Since SWMM is not capable of stream temperature simulation beyond simple mixing. Hydrologic and thermal outputs from SWMM and MINUHET were combined in a hybrid approach that emphasized the strength of each respective model, i.e. SWMM for runoff and streamflow and MINUHET for water temperature. Heat loads were simulated using the MINUHET and the Hybrid models; the Hybrid model (0.56) had a greater NSE than MINUHET (0.45) alone. MINUHET predictions indicated water temperatures would exceed the trout toxicity threshold of 21 °C during 39% and 38% of calibration and validation periods, respectively. Since the observed temperature exceeded the toxicity threshold 59% and 53% of the time for the calibration and validation periods, respectively, MINUHET was not a conservative predictor of the duration of temperatures exceeding the toxicity threshold value.

1. Introduction

Urban development significantly impacts thermal processes within watersheds primarily through the increase in the amount of impervious surfaces due to the construction of buildings and pavement (Cao et al., 2016; Hathaway et al., 2016). These surfaces are typically darker than natural surfaces and absorb and retain thermal energy, thereby raising the temperature of runoff during storm events. Higher temperature runoff directly impacts receiving streams, as stream temperature is an important aspect of water quality and plays a critical role in physical, chemical, and biological processes (Caissie, 2006). Heated runoff from urbanized watersheds is harmful to aquatic organisms, particularly for sensitive species like trout (e.g. *Salvelinus* sp.; Wehrly et al., 2011).

Thermal regimes in streams and rivers are influenced by changes in air and groundwater temperatures, shading, and alterations to the hydrologic regime. These changes occur due to stream and land surface modifications and can be the result of both natural and human activities. The principal anthropogenic influences on stream temperature regime are reduced stream shading and riparian vegetation (Dugdale et al., 2018; Garner et al., 2017; Justice et al., 2017; Loicq et al., 2018), reduced groundwater exchange (Taylor and Stefan, 2009; Wang et al., 2017), increased impervious surface area (Hester and Bauman, 2013; Li et al., 2013), and heat addition from wastewater discharges (Hester and Doyle, 2011).

Available literature documents the increase in stream thermal pollution due to urbanization, providing a rationale for further assessment

* Corresponding author. Hampton Roads Agricultural Research and Extension Center, Virginia Polytechnic Institute and State University, 1444 Diamond Springs Rd, Virginia Beach, VA, 23455, United States.

E-mail addresses: kmehdi87@vt.edu (M. Ketabchy), dsample@vt.edu (D.J. Sample), tthompson@vt.edu (T. Wynn-Thompson), mnyazdi@vt.edu (M. Nayeb Yazdi).

https://doi.org/10.1016/j.jenvman.2018.08.016
Received 9 April 2018; Received in revised form 2 August 2018; Accepted 4 August 2018
Available online 23 August 2018

of thermal effects on aquatic habitat (Herb et al., 2010a,b; Jones and Hunt, 2009; Selbig, 2015; Wardynski et al., 2014). Wehrly et al. (2011) evaluated the sensitivity of brook trout (*Salvelinus fontinalis*) and brown trout (*Salmo trutta*) to daily average and daily maximum stream temperatures. Threshold maximum daily temperature varied from 27.5 °C for a single-day exposure to 25.5 °C for a seven-day exposure; thus, single day maximum temperatures (27.5 °C) can be used as an acute toxicity threshold for trout. Another study indicated that even at very short exposure times (10 min), water at 30 °C could be fatal for trout (Elliott and Elliott, 1995). Many trout species begin to experience some level of stress at approximately 21 °C (Herb et al., 2010a,b; Selbig, 2015). While trout tend to be somewhat resilient to gradual warming with changes in seasons, rapid temperature changes can be fatal (Agersborg, 1930).

Several process-based models and empirical relationships have been developed for simulating streamflow and stormwater temperature from urban areas (Beaufort et al., 2015; Bogan, 2003; Cheng and Wiley, 2016; Laanaya et al., 2017; Mohseni et al., 1998; Mohseni and Stefan, 1999; Morrill et al., 2005; Sapin et al., 2017; Webb et al., 2003). As part of this review, we have identified and categorized each by model characteristics and performance in Table 1. The capability of a model to represent the major processes that govern the surface water thermal regime in the system being modeled is a key consideration when selecting a thermal model (Arrington et al., 2004; Du et al., 2018; Ficklin et al., 2012; Glose et al., 2017). The Hydrologic Simulation Program-Fortran, or HSPF (Bicknell et al., 2001) is a modeling tool that simulates stream temperature and heat load. While the ability of HSPF to simulate runoff and streamflow is significant, there are several drawbacks associated with using HSPF, as outlined in Table 1. In addition to these limitations, the HSPF thermal module (HTRCH) includes numerous parameters, such as the "evaporative coefficient", and the "long-wave radiation coefficient", which need to be calibrated, as they are not typically measured. Calibrating these and other parameters makes it difficult and time-consuming to calibrate the HSPF model for water temperature (Houston Engineering Inc., 2013; James and Xie, 1999).

Of the two models that include temperature routines for both overland and concentrated runoff (Table 1), the Minnesota Urban Heat Export Tool (MINUHET) lacks the shortcomings of many of the recently developed models (Table 1) and is capable of simulating thermal control strategies (TCSs) and overland sheet flow from a wide variety of land covers (Janke et al., 2013). MINUHET is a process-based, sub-hourly model, that can be run as both an event-based and a continuous simulation tool produces time series of runoff temperatures and heat loads at the catchment/pond outlet for 15-min time-steps, thus providing a tool for evaluating the thermal impacts of urban runoff on receiving water bodies (Janke et al., 2013). MINUHET can compute the aforementioned thermal parameters of HSPF (the "evaporative coefficient", and the "long-wave radiation coefficient") based on weather (solar radiation, cloud cover, air temperature, wind speed, relative humidity, etc.) and precipitation input data. The model simulates many types of heat flux, including conduction, convection, and radiation between runoff/stream and air, pervious (forest, grass, agriculture, etc.), and impervious (pavements, roofs, etc.) surfaces, excluding stream bed and groundwater interactions. MINUHET also considers the dominant thermal processes affecting urban reservoirs and ponds, such as advection, in-water turbulent diffusion, shading/sheltering, etc. For these reasons, MINUHET is the most applicable model for simulating thermal regimes in highly urbanized watersheds. One limitation of MINUHET is that the model is not capable of considering point sources of pollution, or domestic or industrial sewerage networks.

In addition to stream/runoff thermal models, several public domain hydrologic models are capable of simulating stream/runoff in urban watersheds, including Hydrologic Modeling Systems, or HMS (Scharffenberg, 2013), HSPF, and the U.S. Environmental Protection Agency Storm Water Management Model, or SWMM (Rossman, 2009). Unlike HMS, which is only a hydrologic model, SWMM is a dynamic hydraulic-hydrologic, employed to simulate stormwater quantity and quality for event-based and continuous scenarios (Niazi et al., 2017; Rossman, 2009); it is widely applied in urban areas. A complete review of its capabilities and deficiencies can be found in Niazi et al. (2017). Furthermore, while HSPF does not require detailed watershed information, such as drainage networks, SWMM is a more physically based model, which makes it ideal to simulate highly urbanized watersheds with intermittent and abrupt storm/stream flow peaks (Ketabchy, 2018; Liu and Tong, 2011; Xie and Lian, 2013). SWMM uses a non-linear reservoir routing method to compute runoff (Palla and Gnecco, 2015; Xing et al., 2016).

The best available runoff/stream thermal tool, MINUHET, has a limited ability to simulate temperature and heat loads for complex urban watersheds (Table 2); such analyses are often performed using SWMM, which was developed primarily for urban watersheds (Palla and Gnecco, 2015; Xing et al., 2016). A comparison of the limitations of MINUHET and SWMM are listed in Table 2. The main limitation of SWMM is the lack of routines to simulate both runoff and stream temperatures. In contrast, MINUHET has limited hydrologic and hydraulic modeling capabilities. For example, MINUHET does not include a comprehensive aquifer module and only supports groundwater-surface water interactions through a basic algorithm of streambed heat flux. Additionally, the number of different saturated hydraulic conductivity values available in MINUHET is limited to only four values (Hydrologic Soil Group, or HSG categories).

Previous thermal evaluation studies (Table 1) have been conducted on larger, predominately pervious watersheds. A gap exists in applications of thermal modeling of urban areas and their associated stormwater conveyance networks and impervious surfaces (roofs and pavement). Although individual MINUHET components have been validated on small watersheds, (Herb, 2008; Janke et al., 2013), to date, MINUHET has not been utilized for continuous simulation of a complex urban watershed including open channels, multiple detention or retention ponds, and a variety of urban land covers. The goal of this research was to assess the impacts of urbanization on stream water temperature through the application of available thermal and hydrologic modeling tools, MINUHET and SWMM, respectively. Stream temperature was assessed with respect to brook trout (*Salvelinus* sp.), a local sensitive fish species; the typical brook trout threshold temperatures for upper avoidance limits or initials stress, and the incipient lethal limit for a seven-day exposure (21 °C and 25.5 °C, respectively), were used to evaluate the simulation (Jones and Hunt, 2009; Selbig, 2015). The models were applied to a medium-sized urban watershed, Stroubles Creek, in Blacksburg, Virginia, and the capabilities of each model were then assessed. Stroubles Creek has several monitoring locations at which streamflow, groundwater level, weather data, and water temperatures have been recorded for several years at the Virginia Tech Stream Research, Education, and Management Lab, or StREAM Lab (StREAM Lab, 2009). While the modeling output time-step was 15 min, MINUHET and SWMM models were developed, calibrated, and validated at hourly and daily time steps using data from two StREAM Lab monitoring stations. Model sensitivity was assessed by comparing both event-based and continuous streamflow estimates. SWMM-simulated streamflow and water temperature from MINUHET were combined to form a unique, hybrid approach to simulate heat export from the watershed (henceforth the "Hybrid model"), and a comparison of the capabilities of MINUHET and the Hybrid model for simulating heat export was conducted. While some event-based simulations of heat export have been conducted (Janke et al., 2013, 2009), few, if any have evaluated thermal loads continuously across a season. The need for simulation of thermal processes within medium-size highly urbanized watersheds has been demonstrated due to the production of large heat loads during summer storm events and their associated potential impacts on aquatic life of downstream water bodies (Jones and Hunt, 2010; Long and Dymond, 2014).

Table 1
Classification of recently developed thermal models in simulation/prediction of stream and surface runoff temperature (ordered by date).

Reference	Model name	Empirical/ Process-based	Runoff temperature simulation	Stream temperature simulation	Event-based/ continuous simulation	Minimum time step duration	TCSs [a] simulation	Model performance applied to case studies	Descriptions
Du et al. (2018)	Modified SWAT[b]-Version 2	Process-based		✓	Both	Daily			Incorporation of an equilibrium temperature approach in to the hydroclimatological model (named as Modified SWAT-Version 1) developed by Ficklin et al. (2012); The equilibrium temperature approach accounts the effect of climate data and water depth to simulate water-air heat transfer; it does not calculate the conduction heat transfer of surface runoff and pervious and impervious surfaces.
Sapin et al. (2017)	NA[c]	Process-based		✓	Continuous	Daily		$0.89 < R^2 < 0.94$	Developed using a K-nearest neighbor bootstrap technique.
Glose et al. (2017)	HFLUX[d]	Process-based		✓	Continuous	NA		RSR = 3–6.2%; RMSE = 0.18–0.40 °C	A deterministic, simple 1-D stream heat budget model (written in MATLAB)[e].
Laanaya et al. (2017)	GAM[f]	Empirical		✓	–	Daily		RMSE = 1.44 °C; bias = −0.04	It is based on modeling the response of water temperature to air temperature and flow, using a sum of nonlinear functions; Proved to have better performance compared to other empirical approaches such as residuals regression, logistic, and linear regression models.
Cheng and Wiley (2016)	RPSTM [g]	Process-based		✓	Continuous	Daily		$0.59 < R^2 < 0.98$	Developed to minimize the high parametrization costs of stream temperature simulation; appropriate when there is no sufficient data.
Beaufort et al. (2015)	NA	Process-based		✓	Continuous	Daily		RMSE = 1.90 °C; Median bias = 0.70 °C	
Janke et al. (2013)	MINUHET	Process-based	✓	✓	Both	15-mi.	Detention/Retention/ Infiltration ponds, rock trench, increase shading and vegetation canopies, cool pavements.	Absolute difference < 1.50 °C	Including a user-friendly graphical user interface (GUI); Applied to a case study of small urban watershed in Plymouth, MN.
Houston Engineering Inc. (2013), James and Xie (1999)	HSPF	Process-based	✓	✓	Both	Hourly		PBIAS = −4.30 - 10.80%	Needs many watershed-related variables to calibrate the thermal module (HTRCH)[h]; does not consider heat washed off by stormwater through pavements; not a hydraulically coupled river temperature model.
Ficklin et al. (2012)	Modified SWAT-Version 1	Process-based		✓	Both	Daily		NSE = 0.81; Mean error = −0.63 °C	Modified the empirical linear regression of stream temperature module of SWAT by adding a simplified contribution (volume) of snowmelt, groundwater, surface runoff, and soil water lateral inflow to streams on daily time-steps; it does not account the heat flux equations of conduction, convection, and radiation between water and air/impervious/ pervious surfaces; developed mainly for highly pervious watersheds.
Herb et al. (2010a,b)	SNTEMP [i]	Process-based		✓	Continuous	Mean daily and max.	The ability to increase shading	RMSE = 0.70–1.90 °C	A steady state (no water or heat storage terms) model.

(continued on next page)

Table 1 (*continued*)

Reference	Model name	Empirical/ Process-based	Runoff temperature simulation	Stream temperature simulation	Event-based/ continuous simulation	Minimum time step duration	TCSs [a] simulation	Model performance applied to case studies	Descriptions
Morrill et al. (2005)	NA	Empirical		✓	–	Mean daily and weekly		NSE = 0.85; RMSE = 2.20 °C	Developed a nonlinear regression between air and stream temperature.
Arrington et al. (2004)	TURM [j]	Process-based	✓		Event-based	5 mi.	Rock cribs and thermal swales [k]	Mean bias = 1–2 °C	Evaluate the impacts of atmospheric and urbanization heat inputs.
Bogan (2003)	NA	Empirical		✓	–	Mean weekly		The slope of fitted line (S) for 156 stream gaging stations (SGTs) was near to 1.0 and S for 440 SGTs was less than 1.0.	Developed a linear regression between mean weekly stream temperature and mean weekly equilibrium temperature[l].
Mohseni and Stefan (1999)	NA	Empirical		✓	–	Mean weekly			Proved the well-accuracy of linear regression (for moderate air temperatures) between stream temperature and air temperature, based on air temperature and equilibrium temperature relationship.
Mohseni et al. (1998)	NA	Empirical		✓	–	Mean weekly		R^2 greater than 0.90 at more than 84% (517) of gaging stations; RMSE = 1.64 ± 0.46 °C	Developed a logistic non-linear regression equation as a function of weekly mean air temperatures.
Webb and Walling (2003)	NA	Empirical		✓	–	Weekly and mean monthly		Correlation coefficient of regressions = 0.90–0.98	Developed a linear regression between weekly and monthly averages of air and stream temperature.

[a] Thermal Control Strategies.
[b] Soil and Water Assessment Tool.
[c] NA: Information Not Available.
[d] HFLUX Stream Temperature Solver.
[e] Streamflow variations are assumed to be due to groundwater discharge, rather than other sources such as tributaries or stormwater, thus making it not appropriate for stream temperature simulation during storm events.
[f] Non-parametric water temperature Generalized Additive Model.
[g] Reduced Parameter Stream Temperature Model.
[h] A drawback of HSPF's approach to modeling stream temperatures is that it assumes complete mixing, which is not realistic particularly when streams are wide and deep; James and Xie (1999) produced a linear regression between simulated temperature and watershed imperviousness using HSPF.
[i] Stream Network Temperature Model.
[j] Thermal Urban Runoff Model.
[k] Rock crib: a bed of rocks receiving stormwater from an urbanized area; thermal swale: a vegetated trench receiving stormwater from an urbanized area.
[l] The stream temperature at which the sum of all heat fluxes through the stream is 0.0.

Table 2
MINUHET and SWMM limitations with respect to hydrologic and thermal simulations.

Model	Limitations
MINUHET	No comprehensive aquifer module.
	Limited to short time series and small watersheds.
	In-channel thermal processes not modeled.
	Atmospheric heat transfer not modeled for routing elements.
	Limited to four values of soil hydraulic conductivity.
SWMM	No capability to model thermal processes beyond simple mixing.

2. Methods and materials

2.1. Site description of the case study

The 58-km^2 Stroubles Creek watershed is located in Montgomery County, Virginia, USA and is a tributary to the New River, part of the Ohio-Mississippi River-Gulf of Mexico system. The subject of this paper is a 14.1 km^2 upstream portion of the Stroubles Creek watershed (Fig. 1a). A monitoring station operated by the Virginia Tech StREAM Lab is located at the watershed outlet as shown on Fig. 1a. Land cover is primarily urbanized (75%), with 21% agricultural and 4% forest, based on the National Land Cover Database (Multi-Resolution Land Use Consortium, 2011). The Duck Pond (Fig. 1a) acts as a divider between the highly urbanized headwater portion (approximately 7.8 km^2 in area) and the downstream agricultural and forested portion of the Stroubles Creek watershed (approximately 6.3 km^2). Central Branch and Webb Branch are two tributaries that merge at the Virginia Tech Duck Pond to form Stroubles Creek (Fig. 1a). Many forms of channel modification exist throughout the watershed, including piped stream reaches, ponds, and channelization. The Town of Blacksburg database (Town of Blacksburg, 2015) and geographic information system (GIS) tool were used to quantify the watershed land use classifications (Table 3 and Fig. 1b). The imperviousness distribution across the watershed was computed by tracing aerial photography (Town of Blacksburg, 2015) and is shown in Fig. 1c. Imperviousness of the entire watershed is 32%, with buildings and parking lots constituting approximately 61% of the total impervious area.

The dominant HSG of the upper watershed is category C (NRCS, 2007), while downstream of Duck Pond the soils are mainly category B, or silt loam and loam (Mostaghimi et al., 2003). The depth to the water table in the downstream portion of the watershed is approximately 1 m and mean annual precipitation is approximately 1030 mm (Hofmeister et al., 2015).

2.2. Data collection

The Town of Blacksburg and Virginia Tech provided storm sewer and surface elevation GIS data. Soil information at the watershed scale was acquired from the Soil Survey Geographic Database (SSURGO) of the Natural Resources Conservation Service (NRCS, 1999). At the StREAM Lab monitoring station, a CS451 pressure transducer (Campbell Scientific Inc., Logan, UT, U.S.A., water level resolution: 0.0035% FS) and a CR1000 datalogger (Campbell Scientific Inc., Logan, UT, U.S.A.) measure and record stream stage every 15 min (Fig. 1a). Stage is converted to discharge using a rating curve, which was developed based on Stroubles Creek historical stage-discharge data. In addition, an YSI Sonde (6920 V2, Xylem Analytics, U.S, ± 0.15 °C) records water temperature. Precipitation is recorded by the Town of Blacksburg and the StREAM Lab meteorological station at 15 min time steps. A tipping bucket rain gage (TR-525USW, Texas Electronics, Inc., Dallas, TX, ± 1%) monitors precipitation at the Town of Blacksburg weather station. Solar radiation, wind speed, relative humidity, and air temperature are measured every 30 min at the StREAM Lab weather station, located approximately 300 m downstream of the Stroubles Creek

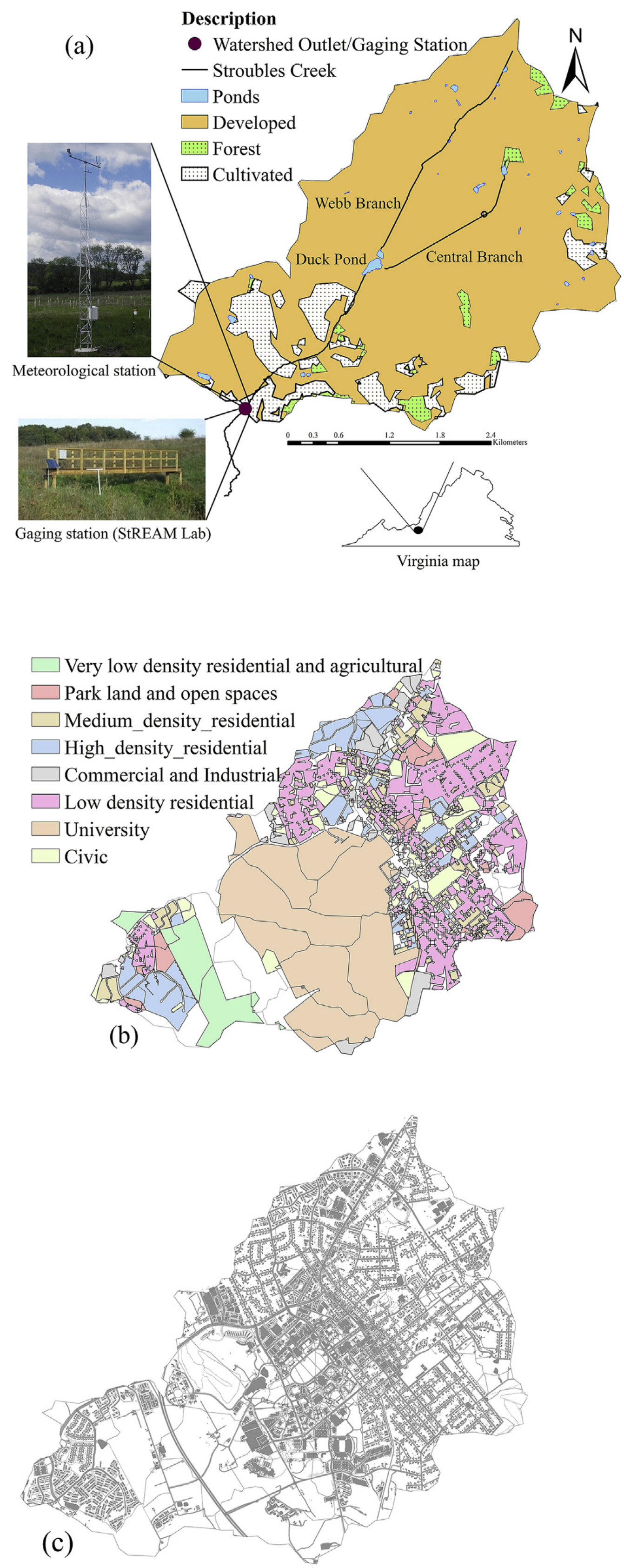

Fig. 1. (a) Land cover map of the Stroubles Creek watershed, with gaging station location; (b) Land use (the white portions of land use map are the lands with other applications); (c) imperviousness distribution (the grey portions of the imperviousness map represent impervious lands).

Table 3
Land use categories of the case study watershed.

Land use type	Percentage
Commercial/Industrial	4.0
Very low density residential and agricultural	12.8
Low density residential	17.1
Medium density residential	4.0
High density residential	7.0
University	25.4
Park land/Opens spaces	3.3
Civic	5.5
Other	20.9

monitoring station (Fig. 1a). The StREAM Lab weather station includes a Campbell Scientific TE525 rain gage (Logan, UT, U.S.A., 1.0% up to 2 in/hr.), a Campbell Scientific 034A/034B anemometer (± 0.1 m/s), a Campbell Scientific CS215 sensor for measuring air temperature and relative humidity (± 2% at 25 °C), and a Campbell Scientific CS300 pyranometer (± 5%) for daily total net radiation measurements. Cloud cover data were acquired at 20-min intervals through the National Oceanic and Atmospheric Administration (NOAA, 2016) The depth to groundwater in the floodplain adjacent to the weather station is measured every 10 min in two piezometers with Campbell Scientific CS451 pressure transducers (water-level resolution: 0.0035% FS).

2.3. SWMM and MINUHET model setup

A total of 43 subwatersheds and 30 detention/retention ponds were delineated within the watershed. The urbanized portion of the watershed (upstream of the Duck Pond) is more complex than the watershed downstream of the Duck Pond due to intensive urban development. Hence, the subwatershed delineation was conducted manually in the urbanized portion of the watershed based on the locations of the ponds and the stormwater drainage network/infrastructure. Downstream of the Duck Pond, elevation data were used to delineate the subwatersheds using the watershed extension GIS application (Ketabchy et al., 2016).

Stroubles Creek was modeled as a pervious open-channel system with irregular cross-sections downstream of the Duck Pond and impervious rectangular cross-sections beneath and upstream of the Virginia Tech campus for both the MINUHET and SWMM configurations. The outlet of each pond was modeled as a weir structure. Routing computations were conducted for each pond, and the stage-storage (bathymetry) characteristics of the ponds were computed using information from the Town of Blacksburg and the watershed digital elevation models (DEMs). Given the fine-grained sediment that has accumulated at the bottom of the stormwater ponds and the relatively steady water levels in the wet ponds, infiltration through the pond bottom was determined as a fixed rate, rather than computed using typical models such as the Green-Ampt model. Tailwater effects at pond outlets were also neglected; this assumption was considered reasonable due to the topography within the watershed.

The Green-Ampt infiltration and dynamic wave methods were used for the infiltration and routing models of SWMM, respectively. The Green-Ampt model is a process-based infiltration model, which makes it more feasible for process-based models such as SWMM (Alamdari et al., 2017; Ficklin and Zhang, 2013; Rosa et al., 2015). The dynamic wave method solves the complete one-dimensional Saint-Venant flow equations and produces the most theoretically accurate runoff results (Alamdari et al., 2017). Groundwater table elevation was quantified using the geological maps of Blacksburg (Geology and Mineral Resources Divison of Commonwealth of Virginia, 1985), and floodplain piezometers at the StREAM Lab. SWMM also computes evaporation through air temperature data using Hargreaves' method (Rossman, 2009). To build the model structure and conduct the sensitivity analysis, PCSWMM (Computational Hydraulics International, 1999) was used to directly import spatial information and attributes from a geodatabase GIS. Although the SWMM and PCSWMM algorithms and routines are the same, PCSWMM provides GIS integration, facilitating model production, as well as a suite of other enhancements.

Unlike SWMM, the hydro-thermal routing model of MINUHET relies solely on the kinematic wave algorithm as the routing module and MINUHET calculates infiltration using the Green-Ampt method (Herb, 2008; Herb et al., 2008). The thermal properties of pervious (forest, grass, agriculture, etc.) and impervious (roofs and pavements) areas including albedo, thermal diffusivity, and surface roughness (Appendix A) were imported in to the MINUHET. The watershed module of MINUHET was used to simulate the time series of runoff temperature for the impervious and pervious sections of each subwatershed. Based on these two simulated time series, the watershed thermal module of MINUHET uses a simple mixing method (based on equilibrium and energy balance approach) to produce a composite hydrograph and time series of runoff temperature an each subwatershed outlet (Herb et al., 2008; Janke et al., 2013).

2.4. Sensitivity analysis

A sensitivity analysis was conducted to assess the influence of individual model input parameters on SWMM and MINUHET streamflow and temperature output (Ahmadisharaf et al., 2016; Kong et al., 2017; Nahvi et al., 2018; Nayeb Yazdi et al., 2015; Stefan et al., 2008). The sensitivity of the following SWMM and MINUHET model outputs were quantified: average total streamflow and streamflow-averaged temperature, throughout the calibration period (summer 2016). The sensitivities of streamflow and temperature to the input parameters can be represented by the sensitivity coefficient, S_r (James and Burges, 1982). The greater the absolute value of S_r, the more sensitive output is to a particular input parameter. Positive values of sensitivity coefficients indicate a direct relationship between the parameters and the outputs, while negative values indicate an inverse relationship. Selected models input parameters and the potential range of values based on literature and field data are shown in Table 4.

2.5. Calibration and validation at the watershed outlet

SWMM and MINUHET inputs were chosen for the model calibration process based on sensitivity analysis, current manuals, field data, model defaults, and literature sources. Measured streamflow at the StREAM Lab between June 15 and Sept. 30 of 2016 and 2015 was selected to represent summer conditions and was used to calibrate and validate the models, respectively; while the modeling output was at 15 min intervals, the models were calibrated on the aggregated hourly time-steps and were assessed on both hourly and daily time-resolution. The study focus was on the summer periods because this is the critical period for temperature in terms of sensitive species, such as trout. To build and run the thermal module of MINUHET, weather data are needed, including solar radiation, air temperature, relative humidity, wind speed, cloudiness, and precipitation. Climate files for the calibration and validation periods were built using 15 min data. The MINUHET model was calibrated for thermal processes by adjusting the pavement heat capacity, thermal diffusivity, and thickness to match observed water temperatures.

2.5.1. Goodness-of-fit criteria

The efficacy of calibration and validation results was evaluated using a group of goodness-of-fit tests: Nash-Sutcliffe Efficiency (NSE) (Nash and Sutcliffe, 1970), percent bias (PBIAS) (Gupta et al., 1999), and root mean squared error (RMSE) or RMSE Standard Ratio (RSR) (Moriasi et al., 2015; Singh et al., 2004). Model fit can also be assessed by fitting a line using linear regression between the predicted and observed values (Bennett et al., 2013). To evaluate model performance, a

Table 4
Ranges of selected models input parameters based on literature and field data.

Parameter	Unit	Value Range	References
SWMM			
Imperviousness	%	± 15% of each subwatershed	Kong et al. (2017)
Hydraulic width	m	± 10% of each subwatershed	Rossman (2009)
Impervious Manning roughness	–	0.01–0.03	Wanielista (1997)
Pervious Manning roughness	–	0.02–0.45	Huber and Dickinson (1988)
Impervious depression storage	mm	0.3–4.0	Huber and Dickinson (1988)
Pervious depression storage	mm	2.5–7.5	Huber and Dickinson (1988)
Saturated hydraulic conductivity	mm/hr.	± 20% of initial values	Huber and Dickinson (1988), and Rossman (2009)
MINUHET			
Heat capacity of pavements	$J/m^3\cdot°C$	$1.9–3.7 \times 10^6$	Kavianipour and Beck (1977)
Thermal diffusivity of pavements	m^2/s	4.42×10^{-7}-14.4×10^{-7}	Luca and Mrawira (2005)
Pavement thickness	m	0.102–0.203	Kavianipour and Beck (1977)
Saturated hydraulic conductivity	m/s	3.61×10^{-7} (HSG: D) -2.75×10^{-5} (HSG: A)	Rawls (2006)
Subwatershed degree of shading	%	± 15% of initial estimate	Aerial photos and field data
Open channel degree of shading	%	± 15% of initial estimate	Aerial photos and field data
Dew point temperature	°C	± 2 °C of initial calculated values	Stefan et al. (2008)

Table 5
Model performance rating system (Moriasi et al., 2015).

Statistical Method	Value Range	Model Performance Rating
R^2	≥0.75	Good
	≥0.6	Satisfactory
	< 0.6	Unsatisfactory
NSE	> 0.70	Good
	> 0.50	Satisfactory
	≤0.50	Unsatisfactory
RSR	≤0.55	Good
	≤0.70	Satisfactory
	> 0.7	Unsatisfactory
PBIAS	≤ ± 10%	Good
	≤ ± 15%	Satisfactory
	> ± 15%	Unsatisfactory

qualitative performance rating system was developed to compare the simulated data set with the observed data set based on the values provided from the aforementioned statistical methods (Moriasi et al., 2015) (Table 5).

The Moriasi et al. (2015) rating system is based on daily simulation performance, while in our study, we used a 15 min time-step, aggregated to hourly and daily for calibration. Performance metrics were calculated using both metrics to facilitate comparison with other studies.

2.6. The Hybrid approach

The purpose of developing the SWMM and MINUHET models was to assess the thermal impact of urbanization on Stroubles Creek. Heat export, which represents the heat content of the streamflow/runoff, is a reliable index for assessing aquatic health responses to temperature impacts from urbanization (Janke et al., 2009). Heat export is defined as a function of temperature and streamflow/runoff in a given time interval (Eq. (1)).

$$H_{exp} = \rho_w C_{P,w} Q (T_{out} - T_{ref}) \tag{1}$$

where H_{exp} = heat export rate, J/s; ρ_w = water density, kg/m^3; $C_{P,w}$ = heat capacity of streamflow/runoff (for water = 4.184 J/(ºC·kg)); Q = the volumetric streamflow/runoff at the watershed outlet, m^3/s; T_{out} = the outlet water temperature, ºC; and, T_{ref} = reference temperature, ºC. Total heat export from a rainfall event is the sum of the heat export for every time interval of the event. The reference temperature, T_{ref}, can be chosen such that the heat load represents the heat load above a specific temperature (e.g. a temperature above which trout experience thermal stress, such as 21 °C). The average streamflow temperatures were between 18 and 19 °C (for the current study), for simulated and observed values, resulting in a negative heat export, assuming a reference temperature of 21 °C. Hence, an arbitrary reference temperature of 17 °C was used to ensure that heat export remained positive during the calibration and validation periods (Janke et al., 2013).

Heat export (load) was simulated using two methods, which are diagrammed in Fig. 2. The first method used MINUHET alone, while the second method utilized a hybrid of the SWMM and MINUHET models. MINUHET calculated heat export at each time step given a pre-determined reference temperature. The Hybrid method used water temperatures from MINUHET and streamflow from SWMM to produce a heat load according to Eq. (1). Rather than develop a de-coupled/integrated model using a "loose-coupling" philosophy and model

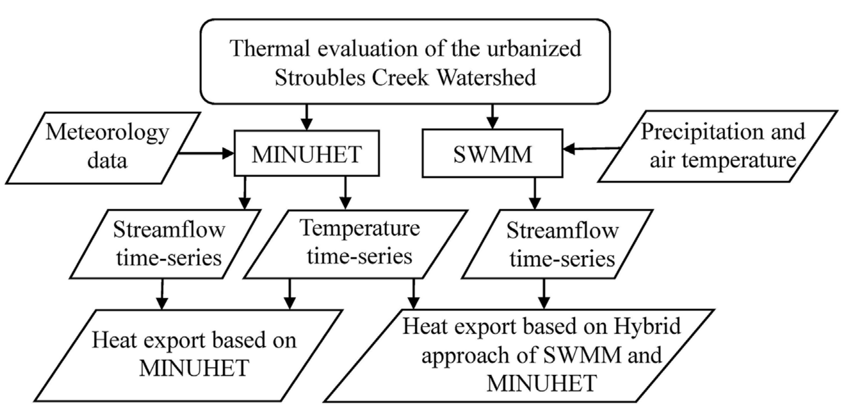

Fig. 2. Diagram of the heat export simulation methods.

integration platforms such as OpenMI (Argent, 2004; Argent et al., 2006; Buahin and Horsburgh, 2015; Leta et al., 2014; Moore and Tindall, 2005; Shrestha et al., 2018, 2013), or importing SWMM outputs (streamflow) as input to the thermal module of MINUHET (Xu et al., 2007), which is not feasible in the current MINUHET configuration, Eq. (1) was utilized to simulate heat export based on SWMM (streamflow) and MINUHET (temperature) outputs. Since the heat loss routines in MINUHET utilize the overland flow rates simulated by MINUHET (i.e. the temperature simulation time series are dependent on MINUHET streamflow simulation), rather than the overland flow rates calculated by SWMM, the Hybrid approach does not fully integrate the two models. It also cannot maintain the heat load balance, a significant limitation. Although the Hybrid approach may have significant uncertainty, it likely improves the accuracy of heat load simulations.

3. Results and discussion

3.1. Sensitivity analysis results

A sensitivity analysis was conducted based on similar studies (Alamdari et al., 2017; Huber and Dickinson, 1988; Kavianipour and Beck, 1977; Luca and Mrawira, 2005; Wanielista, 1997; Xing et al., 2016) and the results are provided in Table 6. The parameters in Table 6 are ordered based on the absolute values of sensitivity level, from high to low. SWMM model runs indicated that the average total streamflow volume was most sensitive to imperviousness (S_r = 0.380), followed by impervious depression storage (S_r = −0.110), and subwatershed hydraulic width (S_r = 0.030). Unlike similar studies (Barco et al., 2008; Rawls, 2006), the SWMM model was not very sensitive to the Green-Ampt infiltration parameters (hydraulic conductivity, S_r = −0.007).

The MINUHET model water temperature predictions were highly sensitive to dew point temperature (S_r = 0.762, calculated from air temperature and relative humidity) compared to other thermal parameters, such as heat capacity and thermal diffusivity of pavements (Table 6). This strong sensitivity was especially true during conditions free of large atmospheric or ground heat fluxes, which commonly occurred early in the morning. One of the key reasons the MINUHET thermal module is sensitive to dew point temperature is because the model assumes the rainfall temperature is equal to the dew point temperature (Janke et al., 2013). The dew point temperature and the pavement heat capacity were the most important parameters affecting water temperature in the MINUHET model. Water temperature was less sensitive to pavement thermal diffusivity and thickness, as compared to the dew point temperature and the pavement heat capacity (Table 6). The MINUHET model average streamflow demonstrated a high sensitivity to saturated hydraulic conductivity (S_r = −0.510), mainly due to the increased magnitude of infiltration from pervious areas, which reduced runoff from the watershed.

Table 6
Sensitivity coefficients of each parameter tested for the SWMM and MINUHET models.

Level of Sensitivity	Parameter	S_r
	SWMM	
High	Imperviousness	0.380
↑	Impervious depression storage	−0.110
	Hydraulic width	0.030
	Pervious Manning roughness	−0.008
	Saturated hydraulic conductivity	−0.007
↓	Pervious depression storage	−0.004
Low	Impervious Manning roughness	0.001
	MINUHET (Temperature)	
High	Dew point temperature	0.762
↑	Heat capacity of pavements	−0.023
	Thermal diffusivity of pavements	−0.009
	Pavement thickness	0.008
↓	Open channels degree of shading	−0.002
Low	Subwatersheds degree of shading	−0.002
	MINUHET (Streamflow)	
	Saturated hydraulic conductivity	−0.510

3.2. Calibration and validation for streamflow

The sensitivity analysis results were used to identify potential parameters for later use in calibrating the SWMM and MINUHET models (Appendix B). A map of each calibrated parameter by subcatchment for both models is provided in Appendix B, Fig. B.2. In MINUHET, the soil saturated hydraulic conductivity (K_{sat}) for each subwatershed is assigned based on the HSG. While the K_{sat} associated with each HSG can be changed, the model is limited to only four K_{sat} values (Table 6 and Fig. B2). The percent impervious area was selected as a calibration parameter due to its sensitivity; in SWMM this parameter actually represents effective impervious, which is difficult to estimate. The assumption in SWMM that each subcatchment is an idealized rectangle introduces some uncertainty. Additional uncertainty may stem from the digitizing aerial photography conducted by the Town of Blacksburg and the StREAM Lab. Calibrated values of the subwatershed percent imperviousness for the SWMM model ranged from 0.07 to 0.68, indicating the wide range of imperviousness within the watershed. Furthermore, there is a similarity between the distribution pattern of calibrated Manning's coefficient for the subwatershed pervious and impervious land within the SWMM model (Appendix B). After calibration, simulated streamflow matched the observed values well for each model for the calibration and validation periods. The goodness-of-fit results (model performance) for the calibration and validation periods are summarized in Table 7.

3.3. Streamflow simulation and comparison of the models

Based on the average percent difference between hourly observed and simulated average streamflow (Table 7), SWMM provided better streamflow estimates than MINUHET. Judging from the relatively high values of NSE and low values of PBIAS, the SWMM model was considered well calibrated and validated for hourly average streamflow estimation at the StREAM Lab (Table 7) monitoring location. Since the value of PBIAS for SWMM was very close to zero during the hourly calibration period, the model was reasonably accurate; however, the negative value of PBIAS during the hourly validation period indicated a slight overestimation bias. Hourly streamflow simulation using SWMM was considered satisfactory based on the RSR index (Table 7). Similarly, the R^2 values of the hourly calibration and validation periods, 0.70 and 0.65, respectively, indicated the model predictions matched the

Table 7
Goodness-of-fit test results for assessing the reliability of calibration and validation streamflow results of SWMM and MINUHET models for daily and hourly time steps.

Statistic	SWMM		MINUHET	
	Calibration	Validation	Calibration	Validation
	Model performance (daily)			
NSE	0.75 (G[a])	0.80 (G)	0.80 (G)	0.70 (G)
R^2	0.81 (G)	0.84 (G)	0.84 (G)	0.71 (S[a])
RSR	0.50 (G)	0.44 (G)	0.44 (G)	0.54 (G)
PBIAS (%)	−0.42 (G)	−12.60 (S)	−13.80 (S)	−16.23 (U[a])
	Model performance (hourly)			
NSE	0.67 (S)	0.65 (S)	0.62 (S)	0.57 (S)
R^2	0.70 (S)	0.65 (S)	0.65 (S)	0.55 (U)
RSR	0.58 (S)	0.58 (S)	0.61 (S)	0.69 (S)
PBIAS (%)	−0.26 (G)	−8.20 (G)	−14.50 (S)	−16.60 (U)

[a] G: Good; S: Satisfactory; U: Unsatisfactory.

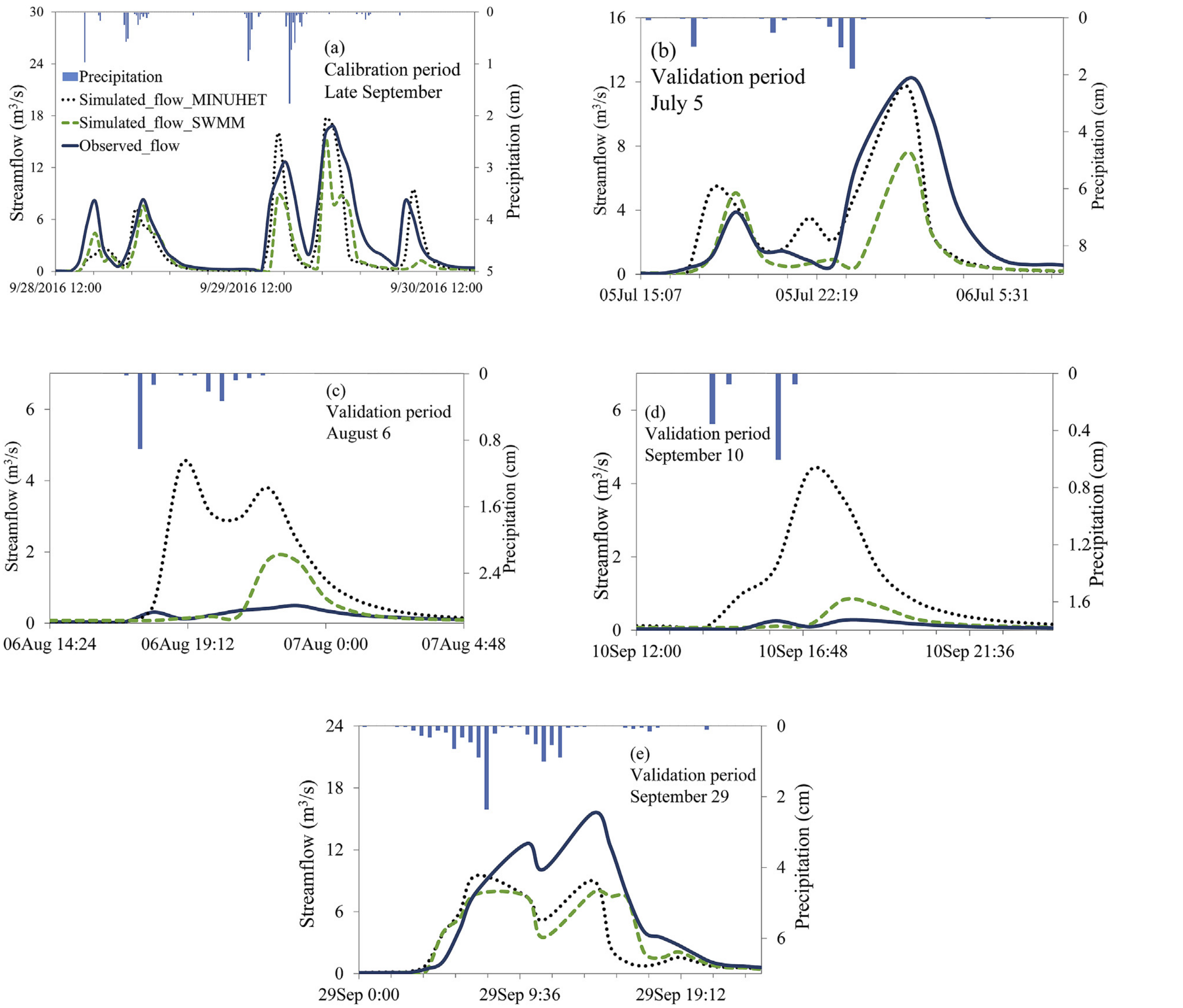

Fig. 3. Comparison of observed streamflow, simulated streamflow by MINUHET and SWMM, for a number of selected storm events during calibration and validation periods (Sim: Simulated, Obs: Observed).

observed values well. Evaluating model performance across events, the SWMM model predicted the observed data set well during the calibration period, but underpredicted streamflow during high intensity storm events in the validation period, e.g., the storm events of July 5 and Sept. 29 (Fig. 3b and e). This underprediction was possibly due to the fact that our criterion was to evaluate all streamflow, including baseflow and storm events, rather than focusing strictly on storm events. In addition, as shown in Fig. 3a, SWMM captured most of the streamflow peaks, particularly the intense storms of late Sept., when a storm event that matched the magnitude of the 10-yr recurrence interval storm occurred.

Based on the values of NSE and PBIAS (Table 7), the MINUHET model calibration and validation were considered “good” for daily streamflow and “satisfactory” for hourly streamflow. The negative value of PBIAS for the hourly calibration and validation periods indicated an overestimation bias. RSR was sufficiently low to receive a satisfactory rating. Simulated and observed values for streamflow were correlated, and R^2 values of the hourly calibration and validation periods were 0.65 and 0.55, respectively. Overall, model streamflow predictions during the calibration and validation periods matched observed values reasonably well (Table 7). In the validation period, MINUHET predicted streamflow reasonably well during intense events with shorter antecedent dry periods prior the storm. Specifically, the verified simulation captured the peak streamflow relatively well during the storm events of July 5 and Sept. 29, 2015 (Fig. 3b and e), but overpredicted peak streamflow for the storm events of Aug. 6 and Sept. 10, 2015 (Fig. 3c and d). Prior to the storm events of Aug. 6 and Sept. 10, 2015, there was little precipitation and longer antecedent dry periods, resulting in high infiltration rates and increased surface storage in the catchment, as compared to the storm events on July 5 and Sept. 29, 2015. In general, SWMM better captured the effects of pervious and impervious depression storage than MINUHET (based on Aug. 6 and Sept. 10 events, Fig. 3c and d).

Goodness-of-fit was assessed by plotting the simulated vs. observed values of streamflow, as illustrated in Fig. 4. The slope of the regression lines in Fig. 4 for the calibration and validation periods are very close to 1.0 for the SWMM model. As shown in Fig. 4a and c, SWMM replicated many of the storm event peaks reasonably well. The slope of the regression line for the MINUHET calibration (Fig. 4b) was close to 1.0, while that for the validation period (Fig. 4d) was less than 1.0 (0.83), indicating stream discharge was underpredicted by MINUHET during the validation period. The errors for hourly streamflow for the calibration and validation of SWMM and MINUHET indicated the errors were lower during dry periods than wet periods. During the storm

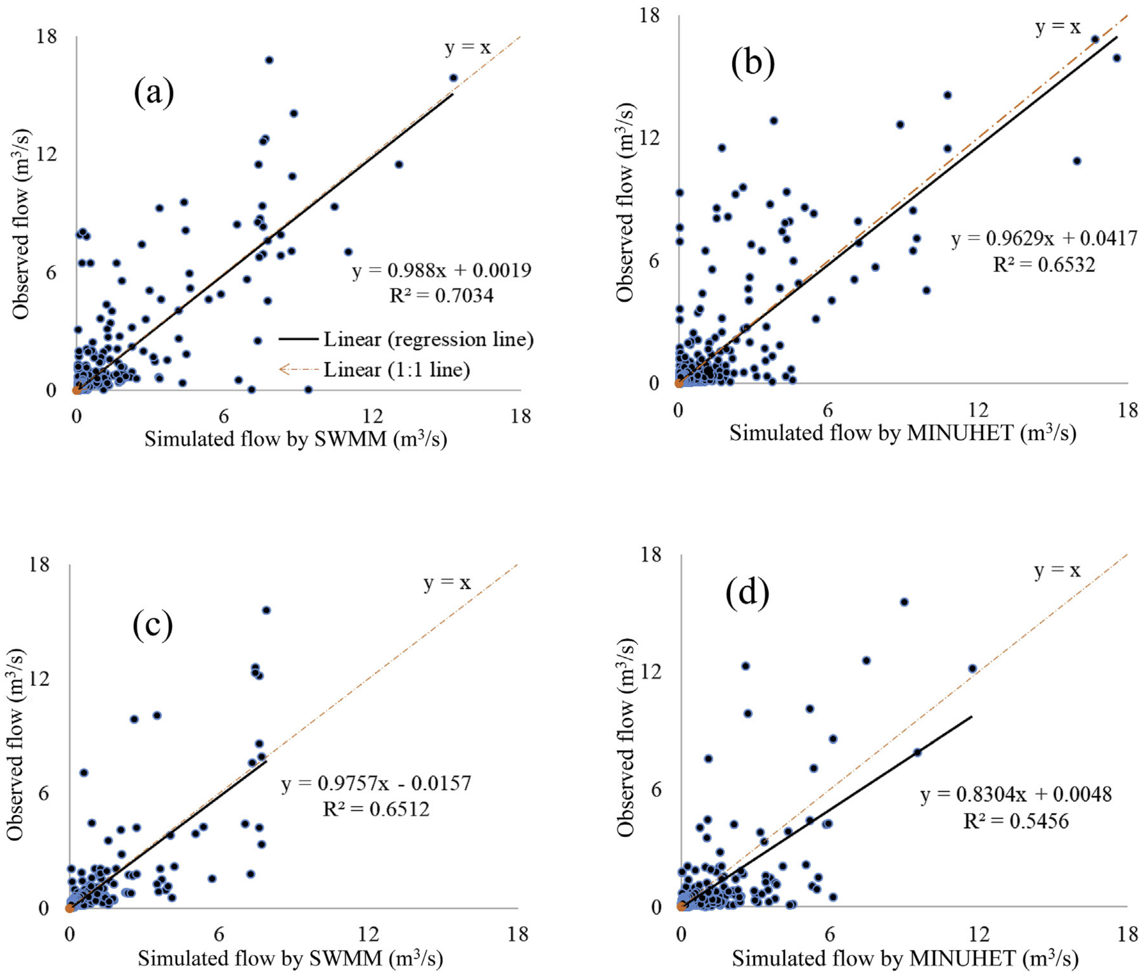

Fig. 4. Scatter plots of observed and simulated hourly streamflow: (a) Calibration for SWMM; (b) Calibration for MINUHET; (c) Validation for SWMM; and (d) Validation for MINUHET.

events of the calibration period, SWMM errors tended to be positive, while the opposite was true for the MINUHET model.

The calibrated and validated models were used to simulate streamflow for a total of ten storm events, as listed in Table 8. Runoff fractions were calculated as the runoff depth divided by rainfall depth. Overall, the SWMM model was a better predictor of runoff fraction than MINUHET for the calibration period. During the less intense storm events of the calibration period, the MINUHET model had a lower computed runoff fraction than SWMM. In contrast, during larger storm events, the MINUHET model predicted much greater runoff fractions than the SWMM model. Moreover, MINUHET had a better peak streamflow response to storm event 5 (approximately a 10-yr rainfall event) than SWMM. SWMM was closer to observed values of runoff fraction for the validation period. During all the storm events of the validation period (Table 8), MINUHET estimated far greater runoff fractions than the runoff fractions obtained from observed data and SWMM model results.

Table 8
Observed runoff fraction and predicted runoff fraction by SWMM and MINUHET, for ten storm events, during the calibration and validation periods.

Storm No.	Storm date	Rainfall Intensity (mm/hr.)	Rainfall Depth (mm)	Runoff Fraction		
				Observed	SWMM	MINUHET
Calibration						
1	7/4/2016	5.9	29.50	0.17	0.14	0.13
2	7/14/2016	7.0	37.60	0.16	0.17	0.12
3	8/3/2016	1.2	39.60	0.13	0.31	0.25
4	8/31/2016	8.4	61.00	0.05	0.05	0.12
5	9/29/2016	3.5	73.15	0.71	0.37	0.63
Validation						
6	7/5/2015	2.5	36.60	0.32	0.23	0.60
7	7/12/2015	1.7	43.70	0.12	0.16	0.18
8	8/10/2015	1.5	13.21	0.37	0.58	0.94
9	9/3/2015	1.3	11.18	0.02	0.04	0.01
10	9/29/2015	4.6	111.7	0.20	0.22	0.48

3.4. Stream temperature simulation using MINUHET

Next, streamflow temperatures at the watershed outlet were simulated using MINUHET. After calibration, the water temperature at the watershed outlet predicted by MINUHET matched reasonably well and satisfactory with the observed values, for daily and hourly simulations, respectively. Goodness-of-fit results for water temperature for the calibration and validation periods are summarized in Table 9 for both daily and hourly simulation performance and the simulated and observed temperatures versus observed and simulated streamflows for two selected storm events during validation periods are shown in Fig. 5. In general, the simulation captured the overall pattern/trend of the observed water temperatures. The absolute value of percent differences of simulated and observed mean temperature (PBIAS) for the calibration period was greater than for the validation period (Table 9).

The MINUHET model was considered satisfactorily calibrated and validated for hourly water temperature and well calibrated and validated for daily water temperature simulation based on NSE and PBIAS.

Table 9
Goodness-of-fit test results for assessing the reliability of calibration and validation results of the MINUHET model for temperature, mean temperature of simulation and observation periods, and temperature error results.

Statistic/Parameter	Calibration	Validation
	Model Performance (daily)	
NSE	0.67 (S)	0.70 (G)
R^2	0.72 (S)	0.91 (G)
RSR	0.57 (S)	0.50 (G)
PBIAS (%)	0.07 (G)	4.70 (G)
	Model Performance (hourly)	
NSE	0.55 (S)	0.58 (S)
R^2	0.70 (S)	0.83 (G)
RSR	0.54 (G)	0.68 (S)
PBIAS (%)	5.60 (G)	4.80 (G)
	Mean Water Temperature (°C)	
Simulated	20.2	19.8
Observed	21.4	20.8
	Average Daily Maximum Water Temperature (°C)	
Simulated	22.0	21.8
Observed	24.0	23.7
	Errors Calculations (°C); Simulated-Observed	
Min error	0.00	0.00
Max error	−5.48	−5.60
Mean error	−1.16	−0.99

The positive values of PBIAS during the calibration and validation periods indicated an underestimation bias. RSR indicated a good calibration and satisfactory validation. In terms of correlation, R^2 values during the hourly calibration and validation periods were 0.70 and 0.83, indicating a satisfactory and a good performance, respectively. Surprisingly, the model performed better in the validation period than in the calibration period, likely because, for the case study conditions, there was strong dependence (sensitivity) of simulated temperature to dew point temperatures.

The factors driving the thermal regime in Stroubles Creek are illustrated by the storm event of Sept. 10, 2015 (Fig. 5a), which had a significant antecedent dry period. During the initial portion of the Sept. 10 storm event (in the afternoon), previously heated and stored water in the Duck Pond was released to the stream. The Duck Pond is the largest pond in the catchment in terms of surface area, and being downstream from most of the urbanized watershed, is ideally situated for capturing peak flows (Fig. 1). However, during this event, a release occurred as a result of the arrival of heated runoff from upstream impervious areas, which mixed with and pushed out the stored, heated water in the Duck Pond, creating the second peak in Fig. 5a; the initial broad temperature rise was due to diurnal temperature changes.

Water temperature at the watershed outlet was primarily influenced by dew point temperature (according to sensitivity analysis results), except during large storm events. The correlation between water temperature at the watershed outlet and dew point temperature was strong at the beginning of high magnitude floods (e.g. Sept. 29 of the validation period), when there was significant surface runoff (Fig. 5b). In this case, there was likely enough surface runoff that any heat absorbed from the pavement was diluted by the large runoff volume and was relatively unaffected by pavement temperature. In addition, as the water vapor in the air condensed, heat energy was released, increasing the rainfall temperature; therefore, the surface water (stream water) temperature and air temperature values became closer during storm events than during dry periods (Fig. 5b). Overall, the dew point and observed and simulated temperatures matched better during flood conditions (defined as high magnitude storm events with runoff overtopping stream banks) than during dry periods (Fig. 5). During floods, the dew point temperature matched the air temperature well since the air was completely saturated (Fig. 5b). In contrast, during the initial hours of lower magnitude storm events (e.g. Sept. 27 of the validation period), water temperature (simulated and observed) was well above dew point temperature since water temperature during baseflow was strongly influenced by the groundwater temperature, which was warmer than the dew point temperature at that time (Fig. 5b).

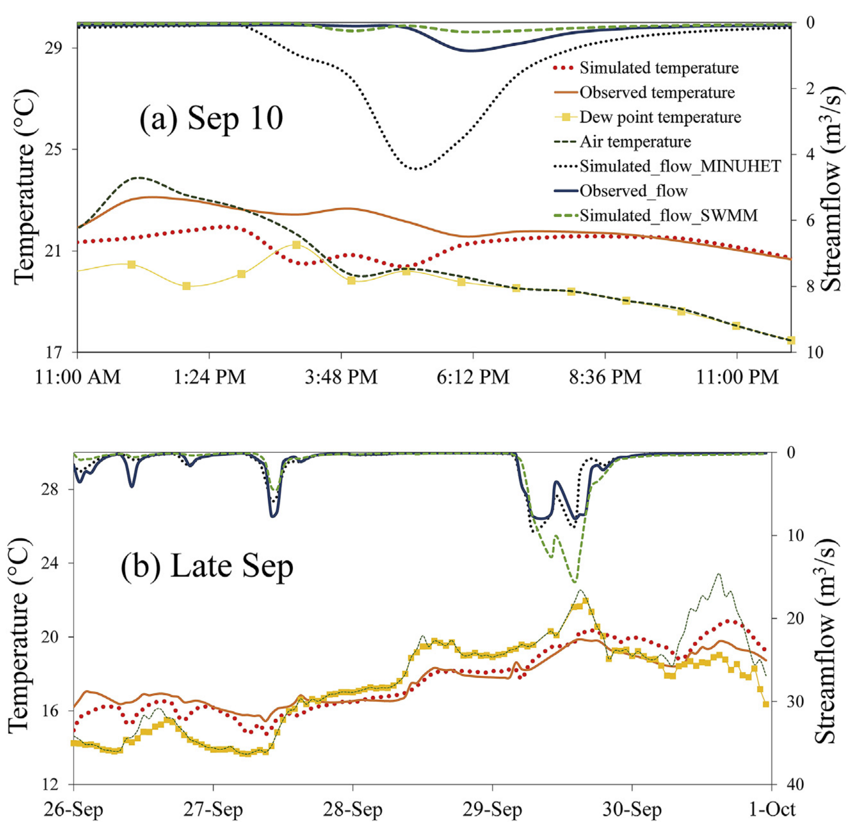

Fig. 5. MINUHET simulated and observed temperatures versus simulated and observed streamflows, for two selected storm events of the validation period.

However, towards the end of the lower magnitude storms, as most of the available heat was absorbed from the ground surface by the runoff, water temperature at the watershed outlet tended to approach dew point temperature, likely because the bulk of the streamflow towards the end of the storm was surface water, rather than groundwater (Fig. 5).

Model performance was also assessed by comparing the simulated vs. observed water temperatures. Looking at the calibration and validation results for temperature simulation (Table 9), the model generally under-predicted water temperature. The mean temperature simulation error during the wet periods and dry periods of the validation time span were −0.78 °C and −1.0 °C, respectively. A similar pattern occurred for the calibration time span, indicating the MINUHET model errors were smaller during wet periods than dry periods.

The MINUHET model simulated the dominant processes controlling Stroubles Creek temperature reasonably well, including advection (associated with streamflow during high flows), conduction (associated with pavements/roofs and runoff interface) and surface heat flux (during low flows). Comparing the simulated versus observed values (Table 9 and Fig. 5), it is apparent that the simulation underestimated water temperature during the calibration and validation periods. This underestimation could be the result of several assumptions made in the model. For example, any errors in the estimation of impervious area would affect partitioning of precipitation between surface runoff and groundwater, resulting in errors in stream temperature predictions. Another consideration is that Blacksburg is located at an elevation of ~670 m; however, the calculation of dew point temperature assumes standard atmosphere (i.e. sea level). This difference could be a source of systematic bias in the calculation of dew point temperature. The under-prediction of water temperature could also have been the result of the model assumption that the temperature of the precipitation was the dew point temperature. As water vapor condenses, it releases energy, which increases the air temperature. Thus, the raindrops are likely warmer than the dew point temperature by the time they reach the ground. This assumption may have been the main reason for the under-prediction of stream temperature by approximately 1 °C throughout the entire calibration and validation periods (Table 9). The errors in stream temperature may also be the result of errors in streamflow prediction, since errors in the volume of streamflow could result in incorrectly modeled stream temperature, even if the remaining heat fluxes were accurately simulated (Fig. 6). During high flows of the validation period when the MINUHET streamflow error was positive, temperature error tended to be negative (underestimation of temperature), while during low flows and reduced streamflow errors, the opposite pattern was observed (Fig. 6).

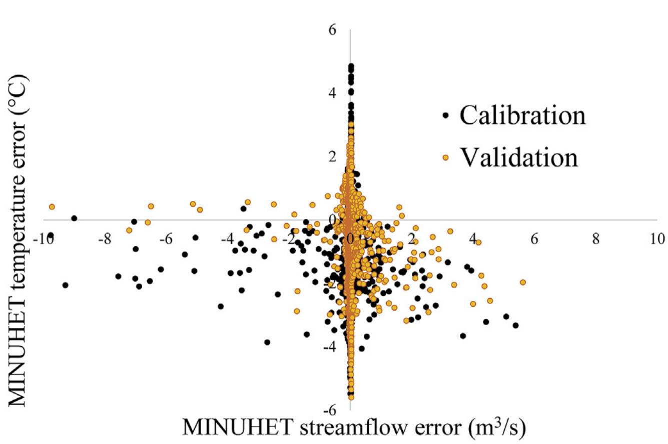

Fig. 6. Temperature error versus MINUHET streamflow error for the calibration and validation periods.

Table 10
Quantile estimation of simulated hourly stream temperature (°C) compared to measured stream temperature, for calibration and validation periods.

Temperature	Percentile								
	1%	5%	10%	25%	50%	75%	90%	95%	99%
	Calibration								
Simulated	14.0	15.9	17.0	18.7	20.3	*21.8*	*23.3*	*24.1*	*25.2*
Observed	15.5	17.5	18.6	19.8	*21.5*	*22.9*	*24.4*	*25.3*	**26.6**
	Validation								
Simulated	11.3	14.7	15.8	18.1	20.2	*21.9*	*23.2*	*24.1*	*25.3*
Observed	11.8	15.7	16.7	19.4	*21.2*	*22.8*	*24.2*	*25.1*	**26.0**

*Bold represents fatal threshold maximum daily temperature for a seven-day exposure (> 25.5 °C), Italic represents initial thermal trout stress (> 21 °C).

3.5. Implications for trout habitats

Stream temperature in summer is the most critical factor affecting the production and distribution of trout species (Selbig, 2015; Wardynski et al., 2014). Brook trout toxicity threshold values of 25.5 °C and 21.0 °C were selected to assess the impact of water temperature on aquatic health (Jones and Hunt, 2009; Selbig, 2015; Wehrly et al., 2011). MINUHET simulated water temperature exceeded the brook trout stress threshold (21.0 °C) during 39% and 38% of calibration and validation periods, respectively, while the observed temperature exceeded the threshold 59% and 53% of the time for the calibration and validation periods, respectively. The model predictions were thus not conservative in identifying the duration of toxicity threshold exceedance. Similar results were observed for the MINUHET models developed by Janke et al. (2013), and Herb (2008). Quantiles of simulated hourly stream temperatures representing the calibration and validation periods were developed (Table 10) to estimate how often water temperatures exceeded the brook trout stress threshold. Similar quantiles for observed hourly stream temperature were developed to compare with the simulated results. Each cell in Table 10 is shaded proportionately according to increasing stress on brook trout as a function of stream temperature. In addition to acute toxicity, thermal stress is also a function of duration of exposure (Wardynski et al., 2014; Wehrly et al., 2011). For simplicity, we will only focus upon acute thermal toxicity using Table 10 as a guideline.

Since quantile estimation of simulated/observed stream temperature represents thermal brook trout stress for at least 25% of the calibration and validation periods (Table 10), restoration of the aquatic habitat of Stroubles Creek should consider potential strategies to mitigate thermal stress to sensitive species by reducing thermal pollution from impervious surfaces. Example of such practices include bioretention cells (Jones and Hunt, 2009), tree canopy restoration for increased shading of streams (Dugdale et al., 2018; Loicq et al., 2018), and installation of light-colored chip seal pavement (Jones et al., 2012).

3.6. Comparison of hydro-thermal streamflow analysis of MINUHET and hybrid models

Total heat export was calculated by the MINUHET and Hybrid models, on an hourly basis, for the calibration and validation periods (Table 11). Since the MINUHET and the Hybrid model's heat export outputs were not calibrated and validated based on observed heat export, the subsequent analysis and discussion on heat export is based upon calibrated streamflow and temperature models. During the calibration period, there was a considerable difference between the simulated and observed heat exports, as the result of a large discrepancy between observed and simulated streamflow and a significant underestimation of streamflow temperature. The simulated total heat export by the Hybrid model was closer to the observed total heat export than MINUHET alone, for both the calibration and validation periods. The

Table 11
Goodness-of-fit test results for assessing the reliability of simulated heat export by Hybrid and MINUHET models and total heat export calculations throughout the calibration and validation periods.

Statistic	Hybrid		MINUHET	
	Calibration	Validation	Calibration	Validation
	Model Performance (hourly)			
NSE	0.62 (S)	0.56 (S)	0.23 (U)	0.45 (U)
R^2	0.63 (S)	0.57 (U)	0.25 (U)	0.46 (U)
RSR	0.63 (S)	0.66 (S)	0.69 (S)	0.74 (U)
PBIAS (%)	20.9 (U)	18.1 (U)	51.5 (U)	36.0 (U)
Total heat export[a] (J)	2.6×10^{13}	1.8×10^{13}	1.6×10^{13}	1.4×10^{13}

[a] Total observed heat export for the calibration and validation periods were 3.3×10^{13} and 2.2×10^{13} J, respectively.

goodness-of-fit results for calibration and validation periods are summarized in Table 11, based on the Moriasi et al. (2015) criteria.

The Hybrid model was satisfactorily calibrated and validated for estimation of heat export based on NSE and R^2 (Table 11). In contrast, the MINUHET model showed poor agreement between simulated and observed heat export for the calibration period (low NSE and R^2), with improved agreement during the validation period (i.e. greater NSE and R^2 compared to the calibration period). The improved model predictions during the validation period are likely due to the better water temperature predictions in the validation period, as compared to the calibration period. RSR was satisfactory for the Hybrid model for calibration and validation; however, MINUHET did not perform satisfactorily for the validation period. The PBIAS positive values indicate that the MINUHET and the Hybrid models both under-predicted observed total heat export. Overall, predicting heat export by the Hybrid model was better than simulating heat export by MINUHET alone (Table 11).

It is apparent that the heat export simulation by the Hybrid model underestimated observed heat export during the calibration and validation periods. The existing percentage difference value (PBIAS) between observed and simulated heat export by the Hybrid model may be due to the existing relatively long open channels (Stroubles Creek) in the watershed, and that MINUHET does not model in-channel thermal processes (Janke et al., 2013). Additionally, there is no atmospheric heat transfer for the routing elements and no junction losses within the MINUHET model, resulting in errors in the temperature simulation (Janke et al., 2009). Since SWMM was calibrated to both baseflow and storm flow, the peak flow rates were underestimated, hence, the simulation using the Hybrid model underestimated observed heat export and can be considered a non-conservative model for medium-sized watersheds. MINUHET was applied to a simple, small watershed (0.05 km^2, 280 times smaller than the current case study) and predicted total heat export with error less than 15% (Janke et al., 2013). In this study, with a much more complex and larger watershed, the MINUHET error was larger (36% for the validation period). The Hybrid model resulted in better percent differences of total heat export than MINUHET alone, for both the calibration and validation periods (Table 11). The percent difference for heat export obtained by the Hybrid model was 18% for the validation period, which is similar to the values simulated by MINUHET in the Janke et al. (2013) study. This finding suggests using the Hybrid model of SWMM and MINUHET for complex urban watersheds with a wide variety of land covers would likely result in better predations of heat export than using MINUHET alone.

4. Conclusions and future work

SWMM and MINUHET are simulation models for routing high-resolution time series of stormwater and heat loads, respectively, through urbanized watersheds. To date, MINUHET has not been evaluated for continuous simulation of an urbanized watershed of the scale of the Stroubles Creek Watershed, approximately 14.1 km^2 in area. In this study MINUHET and SWMM were used to simulate streamflow and thermal effects of the Stroubles Creek watershed as a case study and the strengths of each model (i.e. streamflow for SWMM and temperature for MINUHET) were combined in a unique Hybrid approach to increase the accuracy of heat load simulations. Due to the inclusion of flows generated from SWMM and the heat loads generated from MINUHET, heat load balances could not be maintained. However, the models effectively simulated hourly/daily streamflow, water temperature, and heat load, and predicted the effects of the watershed urbanization on downstream aquatic habitats given trout temperature criteria.

A catchment-based stream temperature model with a subhourly time step and the capability of utilizing a broad range of low impact development (LID) practices is needed to evaluate mitigation measures for water temperature and heat load impairments. LID practices work primarily by infiltrating stormwater and thus could be beneficial in lowering thermal loads in runoff from urban areas. Since SWMM performed better at streamflow simulation, and it has a larger number of LID submodels and a wide user base, we recommend that SWMM be modified to incorporate a thermal modeling capability. This expanded SWMM model could then be utilized to assess the potential for increases in stream heat loads and temperature in any urban watershed and help mitigate changes in land use and climate. In the case of Stroubles Creek, this updated SWMM model would allow changes to the thermal and hydrologic regime stemming from land use or climate changes to be evaluated with respect to thermal toxicity to sensitive species such as brook trout, as well as to provide a means to assess strategies for reducing these impacts.

Declaration of interest

None.

Acknowledgements

Funding for this work was provided in part by the Virginia Agricultural Experiment Station and the Hatch program of the National Institute of Food and Agriculture, U.S. Department of Agriculture. This study was conducted with weather and watershed data provided by the Town of Blacksburg and Virginia Tech StREAM Lab. The authors appreciate the data provided by W. Cully Hession and Laura Lehmann, StREAM Lab director and manager, respectively. The authors would like to acknowledge Erich Hester, and W. Cully Hession, Virginia Tech for their helpful comments. We also thank William Herb, University of Minnesota, as one of the MINUHET model developers, for his guidance throughout the entire project.

Appendix A. Thermal properties of impervious and pervious surfaces

The thermal properties of impervious surfaces (Herb et al., 2010a,b; Janke et al., 2013; Mohajerani et al., 2017; Pomerantz et al., 2003; Thompson et al., 2008; Yazdi et al., 2015) and pervious surfaces (Dugdale et al., 2018; Gartland, 2012; He et al., 2018; Leonardi et al., 2015; Rossman, 2009) of the Stroubles Creek Watershed, which were used as input in to MINUHET model are listed in Tables A1 and A2, respectively. The thermal properties were acquired from the aforementioned literature and during field visit for both type of surfaces.

Table A.1
Thermal properties of pavements and roofs, which were used as input to the MINUHET model.

Surface	Albedo (%)	Thermal Emittance (%)	Surface Roughness	Thermal Diffusivity (m^2/s)	Thickness (m)	Heat Capacity ($J/m^3 \cdot °C$)
Roof	RR[a]: 15 CR[b]: 30	RR: 94 CR: 70	RR: 0.010 CR: 0.010	RR: 10.0×10^{-7} CR: 04.2×10^{-6}	RR: 0.01 CR: 0.02	RR: 3.0×10^6 CR: 3.0×10^6
Asphalt	5	91	0.013	10×10^{-7}	0.20	3.0×10^6
Concrete	35	91	0.011	10×10^{-7}	0.20	3.0×10^6

[a] RR: Residential Roof (Asphalt Shingles).
[b] CR: Commercial Roof (metallic roofing).

Table A.2
Thermal properties of vegetated surface cover, which were used as input to the MINUHET model.

Surface	Albedo (%)	Surface Roughness	Thermal Emittance (%)
Short Grass	21	0.35	0.91
Forest Canopy	16	0.40	0.95
Croplands	20	0.37	0.92

Appendix B. Watershed characteristics and calibration maps as input to the models

The subwatershed characteristics, which were used as input to the calibrated SWMM model are shown in Fig. B1 and Table B1. Input data used for the subwatershed characteristics of the MINUHET watershed module are shown in Table B2. Area, length, width, roughness and slope parameters values used for pervious and impervious lands of SWMM model were used as input for the MINUHET model as well; hence, the parameters mentioned above are not repeated in Table B2. The map of each calibrated parameter by subcatchment for both models is provided in Fig. B2.

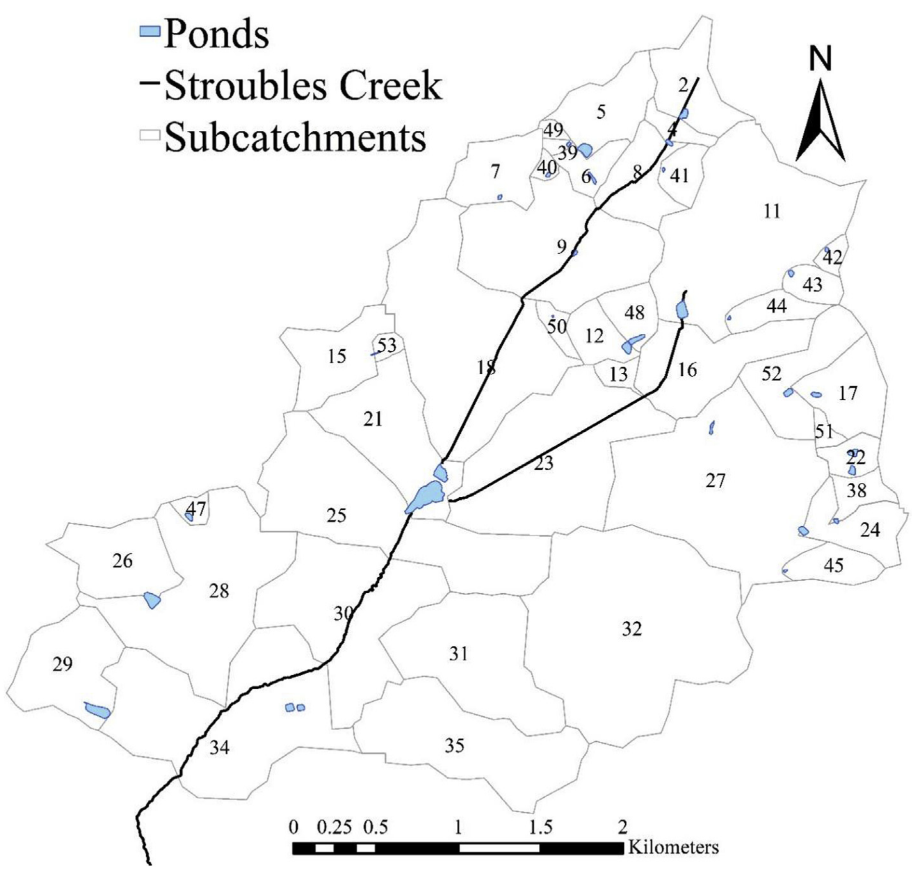

Fig. B.1. The subwatershed delineation; the numbers on each subwatershed represent subwatershed No.

Table B.1
The input watershed parameters for the calibrated SWMM model.

Wat. No.[a]	Area (m^2)	Width (m)	Slope (%)	Imperv. (%)	N Imperv.[a]	N Perv.[a]	Suction Head (cm)	Conductivity (mm/hr.)	Initial Deficit (frac.)
2	2.14×10^5	620	1.12	37	0.010	0.239	16.99	7.87	0.284
4	5.07×10^4	354	1.25	37	0.012	0.342	16.99	6.15	0.284
5	2.21×10^5	271	0.81	53	0.009	0.365	14.00	7.98	0.237
6	8.07×10^4	213	0.94	50	0.013	0.369	16.99	7.29	0.284
7	1.95×10^5	946	0.89	51	0.011	0.348	14.00	9.53	0.237
8	1.94×10^5	304	1.46	26	0.011	0.355	24.00	5.84	0.284
9	6.68×10^5	772	1.10	40	0.013	0.343	24.00	5.94	0.284
11	9.10×10^5	733	1.40	26	0.009	0.220	24.00	4.37	0.284
12	1.04×10^5	203	0.58	41	0.014	0.350	21.50	1.30	0.244
13	3.93×10^4	231	0.46	55	0.010	0.231	24.00	0.81	0.321
15	2.36×10^5	957	0.60	48	0.009	0.339	08.53	20.14	0.147
16	3.63×10^5	583	0.98	32	0.010	0.305	14.00	10.36	0.237
17	2.12×10^5	661	1.74	22	0.014	0.386	6.10	34.34	0.105
18	9.60×10^5	674	0.78	50	0.008	0.245	14.00	7.32	0.237
21	4.24×10^5	551	0.86	29	0.012	0.326	24.00	6.10	0.284
22	7.06×10^4	512	1.18	15	0.012	0.356	09.14	11.46	0.170
23	8.18×10^5	568	0.73	50	0.011	0.218	32.00	0.05	0.378
24	1.74×10^5	1161	1.76	12	0.011	0.291	19.48	4.14	0.264
25	8.04×10^5	930	0.85	30	0.011	0.341	24.00	6.63	0.284
26	2.72×10^5	392	0.83	28	0.013	0.292	07.90	21.16	0.140
27	1.02×10^6	830	0.99	35	0.012	0.329	11.00	12.80	0.190
28	7.56×10^5	541	0.98	21	0.013	0.291	11.00	11.51	0.190
29	3.37×10^5	403	0.96	46	0.013	0.279	14.00	5.87	0.237
30	6.92×10^5	695	0.73	15	0.014	0.354	14.00	6.65	0.237
31	5.60×10^5	605	0.89	24	0.012	0.280	14.00	9.58	0.237
32	1.32×10^6	915	0.80	33	0.013	0.260	12.93	5.16	0.264
34	9.43×10^5	732	0.78	20	0.011	0.366	14.00	11.43	0.237
35	5.93×10^5	510	0.92	10	0.008	0.275	14.00	8.71	0.237
38	6.99×10^4	244	1.80	7	0.009	0.291	12.93	3.25	0.264
39	1.33×10^4	182	0.77	61	0.013	0.300	12.93	3.63	0.264
40	1.96×10^4	294	0.85	43	0.009	0.229	10.29	10.36	0.180
41	7.82×10^4	418	1.29	29	0.008	0.316	14.00	9.98	0.237
42	2.99×10^4	253	1.56	38	0.010	0.262	14.00	6.93	0.237
43	6.78×10^4	240	1.75	31	0.013	0.302	19.48	4.01	0.264
44	9.22×10^4	222	1.50	26	0.008	0.341	11.00	15.21	0.190
45	1.07×10^5	176	0.96	25	0.010	0.364	21.50	1.47	0.244
47	3.16×10^4	200	0.93	44	0.012	0.344	05.97	44.73	0.090
48	9.70×10^4	435	0.80	30	0.010	0.286	21.50	1.40	0.244
49	1.58×10^4	72	0.77	55	0.010	0.274	14.00	7.67	0.237
50	4.06×10^4	110	0.98	68	0.013	0.388	14.00	7.34	0.237
51	2.61×10^4	73	2.02	22	0.014	0.385	06.10	33.81	0.105
52	2.49×10^5	447	1.61	29	0.012	0.366	11.00	8.92	0.190
53	2.43×10^4	141	0.69	62	0.009	0.232	24.00	7.92	0.284

[a] Wat.: Watershed; N Imperv.: Manning's n for impervious area; N Perv.: Manning's n for pervious area.

Table B.2
The input watershed parameters for the calibrated MINUHET model.

Wat. No.[a]	Pervious Land					Impervious Land	
	Shading (%)[b]	Soil Type[c]	Soil moisture status[d]	Vegetation density (%)[e]	Dominant Land use[f]	Shading (%)	Dominant Land use[g]
2	45	C	nor[h]	90	S.G[j]	0	RR[i]
4	15	C	nor	90	S.G	5	RR
5	10	B	nor	100	S.G	10	RR
6	0	C	nor	90	S.G	0	CR[i]
7	0	C	nor	90	S.G	10	RR
8	25	C	nor	70	S.G	10	A[i]

(continued on next page)

Table B.2 (*continued*)

Wat. No.[a]	Pervious Land					Impervious Land	
	Shading (%)[b]	Soil Type[c]	Soil moisture status[d]	Vegetation density (%)[e]	Dominant Land use[f]	Shading (%)	Dominant Land use[g]
9	45	C	nor	90	S.G	0	A
11	50	C	nor	70	S.G	25	RR
12	35	C	nor	90	S.G	10	RR
13	5	C	nor	90	S.G	10	A
15	0	C	nor	100	S.G	0	A
16	15	C	nor	100	S.G	10	A
17	80	C	nor	80	F[j]	20	RR
18	5	C	nor	100	S.G	5	RR
21	0	C	nor	90	S.G	10	A
22	10	C	nor	90	R.C	5	A
23	10	C	nor	90	S.G	15	CR
24	10	C	nor	85	S.G	10	RR
25	0	C	nor	100	S.G	10	CR
26	10	C	nor	60	R.C	0	RR
27	15	C	nor	100	S.G	5	A
28	0	B	nor	80	R.C	5	RR
29	5	B	nor	100	S.G	0	RR
30	5	B	nor	80	R.C	0	CR
31	10	B	nor	80	S.G	10	A
32	15	C	nor	100	S.G	10	CR
34	0	B	nor	80	R.C[j]	0	RR
35	15	B	nor	80	R.C	10	RR
38	10	C	nor	90	R.C	10	C[i]
39	10	C	nor	90	S.G	0	A
40	0	C	nor	100	S.G	0	A
41	10	B	nor	80	S.G	10	CR
42	20	C	nor	90	S.G	10	RR
43	20	C	nor	90	S.G	10	RR
44	15	C	nor	80	S.G	10	A
45	40	C	nor	100	S.G	10	RR
47	15	B	nor	100	S.G	15	A
48	25	C	nor	100	S.G	5	RR
49	10	C	nor	90	S.G	10	RR
50	25	C	nor	90	S.G	5	A
51	10	C	nor	80	S.G	5	A
52	10	C	nor	100	S.G	15	A
53	0	C	nor	100	S.G	0	A

[a] Wat.: Watershed.
[b] The degree of shading from trees and buildings, 0.0 = no shading, 100 = full shading.
[c] USDA hydrologic soil group.
[d] Near surface soil moisture prior to storm events.
[e] The vegetation canopy density, 0.0 = no vegetation, 100 = full vegetation.
[f] The dominant pervious land use for the watershed.
[g] The dominant impervious surface type.
[h] Normal.
[i] RR: Residential Roof, CR: Commercial Roof, A: Asphalt, C: Concrete.
[j] S.G: Short Grass, F: Forest, R.C: Row_Crop.

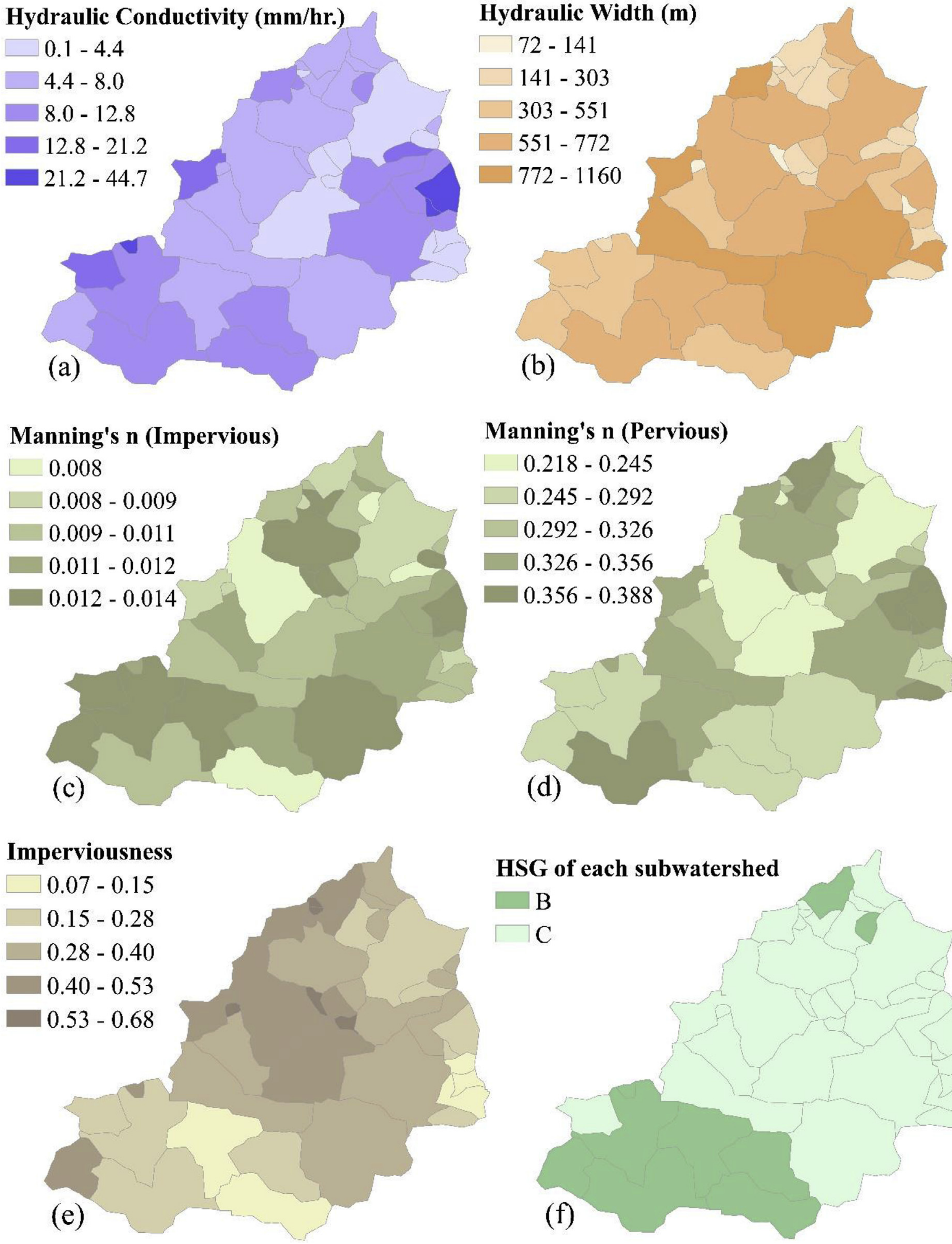

Fig. B.2. Calibrated model parameters by subwatersheds, (a) Hydraulic conductivity for SWMM (mm/hr.); (b) hydraulic width for SWMM (m); (c) Manning's n (of impervious portion) for SWMM; and (d) Manning's n (of pervious portion) for SWMM; (e) Imperviousness for SWMM; and (f) HSG by subwatersheds for MINUHET.

References

Agersborg, H.P.K., 1930. The influence of temperature on fish. Ecology 11, 136–144. https://doi.org/10.2307/1930786.

Ahmadisharaf, E., Tajrishy, M., Alamdari, N., 2016. Integrating flood hazard into site selection of detention basins using spatial multi-criteria decision-making. J. Environ. Plann. Manag. 59, 1397–1417. https://doi.org/10.1080/09640568.2015.1077104.

Alamdari, N., Sample, D., Steinberg, P., Ross, A., Easton, Z., 2017. Assessing the effects of climate change on water quantity and quality in an urban watershed using a calibrated stormwater model. Water 9 Page 464 9, 464. https://doi.org/10.3390/W9070464.

Argent, R.M., 2004. An overview of model integration for environmental applications - components, frameworks and semantics. Environ. Model. Software 19, 219–234. https://doi.org/10.1016/S1364-8152(03)00150-6.

Argent, R.M., Voinov, A., Maxwell, T., Cuddy, S.M., Rahman, J.M., Seaton, S., Vertessy, R.A., Braddock, R.D., 2006. Comparing modelling frameworks - a workshop approach. Environ. Model. Software 21, 895–910. https://doi.org/10.1016/j.envsoft.2005.05.004.

Arrington, K.E., Norman, J.M., Ventura, S.J., 2004. Implementing a Thermal Urban Runoff Model (TURM). https://doi.org/10.14796/JWMM.R220-20.

Barco, J., Wong, K.M., Stenstrom, M.K., 2008. Automatic calibration of the U.S. EPA SWMM model for a large urban catchment. J. Hydraul. Eng. 134, 466–474. https://doi.org/10.1061/(ASCE)0733-9429(2008)134:4(466).

Beaufort, A., Moatar, F., Curie, F., Ducharne, A., Bustillo, V., Thiéry, D., 2015. River temperature modelling by strahler order at the regional scale in the Loire river basin, France. River Res. Appl. 32, 597–609. https://doi.org/10.1002/rra.2888.

Bennett, N.D., Croke, B.F.W., Guariso, G., Guillaume, J.H.A., Hamilton, S.H., Jakeman, A.J., Marsili-Libelli, S., Newham, L.T.H., Norton, J.P., Perrin, C., Pierce, S.A., Robson, B., Seppelt, R., Voinov, A.A., Fath, B.D., Andreassian, V., 2013. Characterising performance of environmental models. Environ. Model. Software 40, 1–20. https://doi.org/10.1016/j.envsoft.2012.09.011.

Bicknell, B.R., Imhoff, J., Kittle Jr., J., Jobes, T., Donigian Jr., A., Johanson, R., 2001. Hydrological Simulation Program–fortran: HSPF, Version 12 User's Manual. AQUA TERRA Consult, Mt. View, Calif. https://doi.org/https://www.epa.gov/exposure-assessment-models/hspf.

Bogan, T., 2003. Stream temperature-equilibrium temperature relationship. Water Resour. Res. 39, 1–12. https://doi.org/10.1029/2003WR002034.

Buahin, C.A., Horsburgh, J.S., 2015. Evaluating the simulation times and mass balance errors of component-based models: an application of OpenMI 2.0 to an urban stormwater system. Environ. Model. Software 72, 92–109. https://doi.org/10.1016/j.envsoft.2015.07.003.

Caissie, D., 2006. The thermal regime of rivers: a review. Freshw. Biol. 51, 1389–1406. https://doi.org/10.1111/j.1365-2427.2006.01597.x.

Cao, Q., Sun, N., Yearsley, J., Nijssen, B., Lettenmaier, D.P., 2016. Climate and land cover effects on the temperature of Puget Sound streams. Hydrol. Process. 30, 2286–2304. https://doi.org/10.1002/hyp.10784.

Cheng, S.-T., Wiley, M.J., 2016. A reduced parameter stream temperature model (RPSTM) for basin-wide simulations. Environ. Model. Software 82, 295–307. https://doi.org/10.1016/J.ENVSOFT.2016.04.015.

Computational Hydraulics International, 1999. PCSWMM. https://doi.org/https://www.pcswmm.com/.

Du, X., Shrestha, N.K., Ficklin, D.L., Wang, J., 2018. Incorporation of the simplified equilibrium temperature approach in a hydrodynamic and water quality model – CE-QUAL-W2. Water Sci. Technol Water Supply ws2018063. https://doi.org/10.2166/ws.2018.063.

Dugdale, S.J., Malcolm, I.A., Kantola, K., Hannah, D.M., 2018. Stream temperature under contrasting riparian forest cover: understanding thermal dynamics and heat exchange processes. Sci. Total Environ. 610–611, 1375–1389. https://doi.org/10.1016/j.scitotenv.2017.08.198.

Elliott, J.M., Elliott, J.A., 1995. The effect of the rate of temperature increase on the critical thermal maximum for parr of Atlantic salmon and brown trout. J. Fish. Biol. 47, 917–919. https://doi.org/10.1111/j.1095-8649.1995.tb06014.x.

Ficklin, D.L., Zhang, M., 2013. A comparison of the curve number and green-ampt models in an agricultural watershed. Trans. ASABE 56, 61–69.

Ficklin, D.L., Luo, Y., Stewart, I.T., Maurer, E.P., 2012. Development and application of a hydroclimatological stream temperature model within the Soil and Water Assessment Tool. Water Resour. Res. 48, 1–16. https://doi.org/10.1029/2011WR011256.

Garner, G., Malcolm, I.A., Sadler, J.P., Hannah, D.M., 2017. The role of riparian vegetation density, channel orientation and water velocity in determining river temperature dynamics. J. Hydrol. 553, 471–485. https://doi.org/10.1016/J.JHYDROL.2017.03.024.

Gartland, L., 2012. Heat Islands; Understanding and Mitigating Heat in Urban Areas. Earthscan, Sterling, VA.

Geology and Mineral Resources Divison of Commonwealth of Virginia, 1985. Geologic Map. https://doi.org/https://www.dmme.virginia.gov/dgmr/mapspubs.shtml.

Glose, A., Lautz, L.K., Baker, E.A., 2017. Stream heat budget modeling with HFLUX: model development, evaluation, and applications across contrasting sites and seasons. Environ. Model. Software 92, 213–228. https://doi.org/10.1016/J.ENVSOFT.2017.02.021.

Gupta, V.H., Sorooshian, S., Yapo, O.P., 1999. Status of automatic calibration for hydrologic models: comparison with multilevel expert calibration. J. Hydrol. Eng. 4, 135–143.

Hathaway, J.M., Winston, R.J., Brown, R.A., Hunt, W.F., McCarthy, D.T., 2016. Temperature dynamics of stormwater runoff in Australia and the USA. Sci. Total Environ. 559, 141–150. https://doi.org/10.1016/j.scitotenv.2016.03.155.

He, T., Wang, D., Qu, Y., 2018. Land surface albedo. In: Comprehensive Remote Sensing. Elsevier, pp. 140–162. https://doi.org/10.1016/B978-0-12-409548-9.10370-7.

Herb, W.R., 2008. Analysis of the Effect of Stormwater Runoff Volume Regulations on Thermal Loading to the Vermillion River. St. Anthony Falls Lab, pp. 1–34 Proj. Reports.

Herb, W.R., Janke, B., Mohseni, O., Stefan, H.G., 2008. MINUHET (Minnesota Urban Heat Export Tool): a Software Tool for the Analysis Fo Stream Thermal Loading by Stormwater Runoff. St. Anthony Falls Lab Proj. Reports).

Herb, W.R., Erickson, T., Stefan, H.G., 2010a. Stream Temperature Modeling of Miller Creek, Duluth, Minnesota. St. Anthony Falls Laboratory Project Reports, Minnesota Pollution Control Agency. https://doi.org/http://www.lakesuperiorstreams.org/archives/miller/MillerEricksonHerbStefanFlowRep_No536-Jan2010.pdf.

Herb, W.R., Janke, B., Mohseni, O., Stefan, H.G., 2010b. MINUHET (Minnesota Urban Heat Export Tool) User Manual.

Hester, E.T., Bauman, K.S., 2013. Stream and retention pond thermal response to heated summer runoff from urban impervious surfaces. J. Am. Water Resour. Assoc. 49, 328–342. https://doi.org/10.1111/jawr.12019.

Hester, E.T., Doyle, M.W., 2011. Human impacts to river temperature and their effects on biological processes: a quantitative synthesis. J. Am. Water Resour. Assoc. 47, 571–587. https://doi.org/10.1111/j.1752-1688.2011.00525.x.

Hofmeister, K.L., Cianfrani, C.M., Hession, W.C., 2015. Complexities in the stream temperature regime of a small mixed-use watershed, Blacksburg, VA. Ecol. Eng. 78, 101–111. https://doi.org/10.1016/j.ecoleng.2014.05.019.

Houston Engineering Inc., 2013. Buffalo River Watershed HSPF Modeling. Houston. https://doi.org/https://www.pca.state.mn.us/sites/default/files/wq-iw5-06q.pdf.

Huber, W.C., Dickinson, R.E., 1988. Storm Water Management Model , Version 4: User's Manual 720. https://doi.org/EPA/600/3-88/001a.

James, L., Burges, S., 1982. Selection, calibration, and testing of hydrologic models. Hydrol. Model. Small Watersheds.

James, W., Xie, J.D.M., 1999. Modeling Thermal Enrichment of Streams Due to Solar Heating of Local Urban Stormwater. Ch 8. pp. 139–157. https://doi.org/10.14796/JWMM.R204-08.

Janke, B.D., Herb, W.R., Mohseni, O., Stefan, H.G., 2009. Simulation of heat export by rainfall-runoff from a paved surface. J. Hydrol. 365, 195–212. https://doi.org/10.1016/j.jhydrol.2008.11.019.

Janke, B.D., Herb, W.R., Mohseni, O., Stefan, H.G., 2013. Case study of simulation of heat export by rainfall runoff from a small urban watershed using MINUHET. J. Hydrol. Eng. 18, 995–1006.

Jones, M., Hunt, W., 2009. Bioretention impact on runoff temperature in trout sensitive waters. J. Environ. Eng. 577–585. https://doi.org/10.1061/41009(333)80.

Jones, M.P., Hunt, W.F., 2010. Effect of storm-water wetlands and wet ponds on runoff temperature in trout sensitive waters. J. Irrig. Drain. Eng. 136, 656–661. https://doi.org/doi:10.1061/(ASCE)IR.1943-4774.0000227.

Jones, M.P., Hunt, W.F., Winston, R.J., 2012. Effect of urban catchment composition on runoff temperature. J. Environ. Eng. 138, 1231–1236. https://doi.org/doi:10.1061/(ASCE)EE.1943-7870.0000577.

Justice, C., White, S.M., McCullough, D.A., Graves, D.S., Blanchard, M.R., 2017. Can stream and riparian restoration offset climate change impacts to salmon populations? J. Environ. Manag. 188, 212–227. https://doi.org/10.1016/J.JENVMAN.2016.12.005.

Kavianipour, A., Beck, J.V., 1977. Thermal property estimation utilizing the Laplace transform with application to asphaltic pavement. Int. J. Heat Mass Transf. 20, 259–267. https://doi.org/10.1016/0017-9310(77)90212-5.

Ketabchy, M., 2018. Thermal Evaluation an Urbanized Watershed Using SWMM and MINUHET: a Case Study of Stroubles Creek Watershed. Virginia Tech, Blacksburg, VA.

Ketabchy, M., Yazdi, M., Ahmadisharaf, E., 2016. An overview on geographic information system (GIS) application in environmental management, case study of algae growth assessment in Tampa Bay. Casp. Sea J. 10, 08–13.

Kong, F., Ban, Y., Yin, H., James, P., Dronova, I., 2017. Modeling stormwater management at the city district level in response to changes in land use and low impact development. Environ. Model. Software 95, 132–142. https://doi.org/https://doi.org/10.1016/j.envsoft.2017.06.021.

Laanaya, F., St-Hilaire, A., Gloaguen, E., 2017. Water temperature modelling: comparison between the generalized additive model, logistic, residuals regression and linear regression models. Hydrol. Sci. J. 62, 1078–1093. https://doi.org/10.1080/02626667.2016.1246799.

Leonardi, S., Magnani, F., Nolè, A., Van Noije, T., Borghetti, M., 2015. A global assessment of forest surface albedo and its relationships with climate and atmospheric nitrogen deposition. Global Change Biol. 21, 287–298. https://doi.org/10.1111/gcb.12681.

Leta, O.T., Shrestha, N.K., de Fraine, B., van Griensven, A., Bauwens, W., 2014. Integrated water quality modelling of the river Zenne (Belgium) using OpenMI. In: Advances in Hydroinformatics. Springer Singapore, Singapore, pp. 259–274. https://doi.org/10.1007/978-981-4451-42-0_22.

Li, H., Harvey, J.T., Holland, T.J., Kayhanian, M., 2013. Corrigendum: the use of reflective and permeable pavements as a potential practice for heat island mitigation and stormwater management. Environ. Res. Lett. 8, 049501. https://doi.org/10.1088/1748-9326/8/4/049501.

Liu, Z., Tong, S.T.Y., 2011. Using HSPF to model the hydrologic and water quality impacts of riparian land-use change in a small watershed. J. Environ. Inf. 17, 1–14. https://doi.org/10.3808/jei.201100182.

Loicq, P., Moatar, F., Jullian, Y., Dugdale, S.J., Hannah, D.M., 2018. Improving representation of riparian vegetation shading in a regional stream temperature model using LiDAR data. Sci. Total Environ. 624, 480–490. https://doi.org/10.1016/J.SCITOTENV.2017.12.129.

Long, D.L., Dymond, R.L., 2014. Thermal pollution mitigation in cold water stream watersheds using bioretention. J. Am. Water Resour. Assoc. 50, 977–987. https://doi.org/10.1111/jawr.12152.

Luca, J., Mrawira, D., 2005. New measurement of thermal properties of superpave asphalt concrete. J. Mater. Civ. Eng. ASCE 17, 72–79. https://doi.org/10.1061/(ASCE)0899-1561(2005)17.

Mohajerani, A., Bakaric, J., Jeffrey-Bailey, T., 2017. The urban heat island effect, its causes, and mitigation, with reference to the thermal properties of asphalt concrete. J. Environ. Manag. 197, 522–538. https://doi.org/https://doi.org/10.1016/j.jenvman.2017.03.095.

Mohseni, O., Stefan, H., 1999. Stream temperature air temperature relationship: a physical interpretation. J. Hydrol. 218, 128–141. https://doi.org/10.1016/S0022-1694(99)00034-7.

Mohseni, O., Stefan, H.G., Erickson, T.R., 1998. A nonlinear regression model for weekay stream temperatures. Water Resour. Res. 34, 2685–2692. https://doi.org/10.1029/

98WR01877.
Moore, R.V., Tindall, C.I., 2005. An overview of the open modelling interface and environment (the OpenMI). Environ. Sci. Pol. 8, 279–286. https://doi.org/10.1016/j.envsci.2005.03.009.
Moriasi, D.N., Gitau, M.W., Pai, N., Daggupati, P., 2015. Hydrologic and water quality models: performance measures and evaluation criteria. Trans. ASABE 58, 1763–1785. https://doi.org/10.13031/trans.58.10715.
Morrill, J.C., Bales, R.C., Conklin, M.H., 2005. Estimating stream temperature from air temperature: implications for future water quality. J. Environ. Eng. 131, 139–146. https://doi.org/10.1061/(asce)0733-9372(2005)131:1(139).
Mostaghimi, S., Benham, B., Brannan, K., Dillaha, T.A., Wagner, R., Wynn, J., Y. G, Zeckoski, R., 2003. Benthic TMDL for Stroubles Creek in Montgomery County. (Virginia).
Multi-Resolution Land Use Consortium, 2011. National Land Cover Database (NLCD). https://doi.org/http://www.mrlc.gov/nlcd11_data.php.
Nahvi, A., Daghighi, A., Nazif, S., 2018. The environmental impact assessment of drainage systems: a case study of the Karun river sugarcane development project. Arch. Agron. Soil Sci. 64, 185–195. https://doi.org/10.1080/03650340.2017.1340641.
Nash, J.E., Sutcliffe, J.V., 1970. River flow forecasting through conceptual models Part I-a discussion of principles. J. Hydrol. 10, 282–290. https://doi.org/10.1016/0022-1694(70)90255-6.
Nayeb Yazdi, M., Delavarrafiee, M., Arhami, M., 2015. Evaluating near highway air pollutant levels and estimating emission factors: case study of Tehran, Iran. Sci. Total Environ. 538, 375–384. https://doi.org/10.1016/j.scitotenv.2015.07.141.
Niazi, M., Nietch, C., Maghrebi, M., Jackson, N., Bennett, B.R., Tryby, M., Massoudieh, A., 2017. Storm water management model: performance review and gap analysis. J. Sustain. Water Built Environ. 3, 04017002. https://doi.org/10.1061/JSWBAY.0000817.
NOAA, 2016. National Oceanic and Atmospheric Administration. National Climate Data Center. https://doi.org/https://www.ncdc.noaa.gov/cdo-web/.
NRCS, 1999. SSURGO. https://doi.org/https://websoilsurvey.sc.egov.usda.gov/App/HomePage.htm.
NRCS, 2007. National Engineering Handbook Chapter 7 Hydrologic Soil Groups. United States Department of Agriculture. https://doi.org/https://directives.sc.egov.usda.gov/OpenNonWebContent.aspx?content=17757.wba.
Palla, A., Gnecco, I., 2015. Hydrologic Modeling of Low Impact Development Systems at the Urban Catchment Scale. https://doi.org/10.1016/j.jhydrol.2015.06.050.
Pomerantz, M., Akbari, H., Chang, S.-C., Levinson, R., Pon, B., 2003. Examples of Cooler Reflective Streets for Urban Heat-island Mitigation: Portland Cement Concrete and Chip Seals. Berkeley, CA 94720.
Rawls, W.J., 2006. Infiltration Properties, second ed. Taylor and Francis, Boca Raton, FL.
Rosa, D.J., Clausen, J.C., Dietz, M.E., 2015. Calibration and verification of SWMM for low impact development. JAWRA J. Am. Water Resour. Assoc. 51, 746–757. https://doi.org/10.1111/jawr.12272.
Rossman, L.A., 2009. Storm Water Management Model: User's Manual. https://doi.org/https://www.epa.gov/water-research/storm-water-management-model-swmm.
Sapin, J., Rajagopalan, B., Saito, L., Caldwell, R.J., 2017. A K-Nearest neighbor based stochastic multisite flow and stream temperature generation technique. Environ. Model. Software 91, 87–94. https://doi.org/10.1016/J.ENVSOFT.2017.02.005.
Scharffenberg, W.A., 2013. Hydrologic Modeling System HEC-HMS 1–442. https://doi.org/http://www.hec.usace.army.mil/software/hec-hms/downloads.aspx.
Selbig, W.R., 2015. Simulating the effect of climate change on stream temperature in the Trout Lake Watershed, Wisconsin. Sci. Total Environ. 521–522, 11–18. https://doi.org/10.1016/j.scitotenv.2015.03.072.
Shrestha, N.K., Leta, O.T., De Fraine, B., van Griensven, A., Bauwens, W., 2013. OpenMI-based integrated sediment transport modelling of the river Zenne, Belgium. Environ. Model. Software 47, 193–206. https://doi.org/10.1016/j.envsoft.2013.05.004.
Shrestha, N.K., Punzal, C., Leta, O.T., 2018. Trace Metal Modelling of a Complex River Basin Using the Suite of Models Integrated in the OpenMI Platform. https://doi.org/10.3390/environments5040048.
Singh, J., Knapp, H.V., Arnold, J.G., Demissie, M., 2004. Hydrologic modeling of the iroquois river watershed using HSPF and SWAT. J. Am. Water Resour. Assoc. 41, 343–360. https://doi.org/10.1111/j.1752-1688.2005.tb03740.x.
Stefan, H.G., Herb, W.R., Janke, B., Mohseni, O., Stefan, H.G., 2008. Thermal pollution of streams by runoff from paved surfaces. Hydrol. Process. 22, 987–999. https://doi.org/10.1002/hyp.6986.
StREAM Lab, 2009. Stream Research, Education, and Management Lab (StREAM Lab). Virginia Tech. https://doi.org/https://www.bse.vt.edu/research/facilities/StREAM_Lab.html.
Taylor, C.A., Stefan, H.G., 2009. Shallow groundwater temperature response to climate change and urbanization. J. Hydrol. 375, 601–612. https://doi.org/10.1016/j.jhydrol.2009.07.009.
Thompson, A.M., Kim, K., Vandermuss, A.J., 2008. Thermal characteristics of stormwater runoff from asphalt and sod surfaces. J. Am. Water Resour. Assoc. 44, 1325–1336. https://doi.org/10.1111/j.1752-1688.2008.00226.x.
Town of Blacksburg, 2015. Blacksburg GIS Database. https://doi.org/http://www.gis.lib.vt.edu/gis_data/Blacksburg/GISPage.html.
Wang, P., Pozdniakov, S.P., Vasilevskiy, P.Y., 2017. Estimating groundwater-ephemeral stream exchange in hyper-arid environments: field experiments and numerical simulations. J. Hydrol. 555, 68–79. https://doi.org/10.1016/J.JHYDROL.2017.10.004.
Wanielista, M.P., 1997. Hydrology and Water Quality Control, second ed. Wiley, New York.
Wardynski, B.J., Winston, R.J., Line, D.E., Hunt, W.F., 2014. Metrics for assessing thermal performance of stormwater control measures. Ecol. Eng. 71, 551–562. https://doi.org/10.1016/j.ecoleng.2014.07.068.
Webb, B.W., Clack, P.D., Walling, D.E., 2003. Water-air temperature relationships in a Devon river system and the role of flow. Hydrol. Process. 17, 3069–3084. https://doi.org/10.1002/hyp.1280.
Webb, B.W., Walling, D.E., 1992. Long term water temperature behaviour and trends in a Devon, UK, river system. Hydrol. Sci. J 37, 567–580. https://doi.org/10.1080/02626669209492624.
Wehrly, K., Wang, L., Mitro, M., 2011. Field-based estimates of thermal tolerance limits for trout: incorporating exposure time and temperature fluctuation. Trans. Am. Fish. Soc. 136, 365–374. https://doi.org/10.1577/T06-163.1.
Xie, H., Lian, Y., 2013. Uncertainty-based evaluation and comparison of SWAT and HSPF applications to the Illinois River Basin. J. Hydrol. https://doi.org/10.1016/j.jhydrol.2012.12.027.
Xing, W., Li, P., Cao, S., Gan, L., Liu, F., Zuo, J., 2016. Layout effects and optimization of runoff storage and filtration facilities based on SWMM simulation in a demonstration area. Water Sci. Eng. 9, 115–124. https://doi.org/https://doi.org/10.1016/j.wse.2016.06.007.
Xu, Z., Godrej, A.N., Grizzard, T.J., 2007. The hydrological calibration and validation of a complexly-linked watershed–reservoir model for the Occoquan watershed, Virginia. J. Hydrol. 345, 167–183. https://doi.org/10.1016/J.JHYDROL.2007.07.015.
Yazdi, M.N., Ketabchy, M., Nia, M.Y., 2015. Clogging evaluation and pollutants removal from surface runoff by permeable pavement system: Insights from the laboratory rainfall simulator. J. UMP Soc. Sci. Technol. Manag. 3.